IEEE Access
Multidisciplinary ⋮ Rapid Review ⋮ Open Access Journal

Received 20 October 2022, accepted 7 November 2022, date of publication 10 November 2022, date of current version 21 November 2022.

Digital Object Identifier 10.1109/ACCESS.2022.3221415

RESEARCH ARTICLE

Two-Degree-of-Freedom Controller Design Based on a Data-Driven Estimation Approach

TATSUNARI SAKAI[1], SHUICHI YAHAGI[2], AND ITSURO KAJIWARA[1]
[1]Division of Human Mechanical Systems and Design, Hokkaido University, Sapporo, Hokkaido 060-8628, Japan
[2]6th Research Department, ISUZU Advanced Engineering Center, Ltd., Fujisawa, Kanagawa 252-0881, Japan
Corresponding author: Shuichi Yahagi (shuichi_yahagi@isuzu.com)

ABSTRACT Data-driven control design is a method to create and tune controllers directly from the initial experimental data without a mathematical model to be controlled. Tracking and disturbance suppression are necessary to control real systems. A two-degree-of-freedom (2DOF) control system is effective to simultaneously enhance the performances of both. This study proposes a direct data-driven tuning method for the controller parameters of a 2DOF control system using only one-shot initial experimental data without mathematical modeling of the controlled object. The proposed approach improves the tracking and disturbance suppression performances by utilizing an estimation method in which the sensitivity function and the closed-loop transfer function are identified after updating the parameters in the time domain. Specifically, the closed-loop response and control input are estimated after updating the parameters, realizing efficient control system design because the control performance can be evaluated prior to implementation. To validate the effectiveness of the proposed method, a simulation for a mechanical system and an experiment for motor control are performed. The proposed method can estimate the response and control input of a 2DOF control system after updating the parameters by offline computations. The optimal control parameters can be obtained to enhance the tracking and disturbance suppression performances.

INDEX TERMS Data-driven control, parameter tuning, two-degree-of-freedom controller.

I. INTRODUCTION

As the number of electronic devices in industry grows, the number of controllers has rapidly increased. The control parameters must be tuned to realize the desired control performance. Usually, this is a trial-and-error tuning process, which requires a lot of experimentation and technical knowledge. However, trial-and-error is costly and depends on individual skills [1], [2]. Another approach is model-based control using a mathematical model of the controlled object. Issues with model-based control include system identification difficulties and controlling performance degradation due to modeling errors [3], [4], [5].

Consequently, studies on model-free control and data-driven control (DDC) are attracting attention [1], [2], [3], [4], [5], [6], [7], [8], [9], [10], [11], [12], [13], [14], [15], [16], [17], [18], [19], [20], [21], [22], [23], [24], [25], [26], [27], [28], [29], [30], [31], [32], [33], [34], [35], [36], [37], [38]. DDC methods design and tune controllers directly from experimental data without a mathematical model of the controlled object. Examples include Iterative Feedback Tuning (IFT) [10], Correlation-based Tuning (CbT) [11], Noniterative Correlation-based Tuning (NCbT) [12], Virtual Reference Feedback Tuning (VRFT) [13], [14], [15], and Fictitious Reference Iterative Tuning (FRIT) [16]. Especially, NCbT [12], VRFT [14], and FRIT [16] can automatically obtain optimal control parameters for linear time-invariant (LTI) systems with an offline computation using only one-shot input/output data of the controlled object. The development cost can be significantly reduced because the optimal control parameters can be obtained without repeated experiments or trial-and-error. Hence, DDC methods are currently applied to many industrial systems [17], [18], [19], [20], [21], [22], [23], [24], [25].

To control real systems, both tracking and disturbance suppression are necessary. A two-degree-of-freedom (2DOF)

The associate editor coordinating the review of this manuscript and approving it for publication was Wonhee Kim.

control system can simultaneously enhance the performances of both. FRIT-2DOF [26], [27] and VRFT-2DOF [28] have been extended to 2DOF control systems. Although FRIT-2DOF [26] can enhance the tracking performance by updating only the feedforward control parameters, it cannot enhance the disturbance suppression performance because the feedback control parameters are fixed. Reference [27] proposed FRIT to enhance the feedback characteristics of closed-loop systems by updating both the feedforward and feedback controllers. However, FRIT-2DOF [27] requires two experiments under different conditions. VRFT-2DOF [28] can simultaneously enhance the tracking and disturbance suppression performance by tuning the feedforward and feedback control parameters, but two prefilters based on the power spectral density of the input signal must be obtained for optimality. In addition, Virtual Internal Model Tuning (VIMT) [29] has recently been proposed. VIMT extended to 2DOF control system [30] can simultaneously enhance the response and feedback characteristics of a closed-loop system with only one update calculation. However, the optimal parameters obtained by VIMT [29], [30] are not unique because they depend on the initial experimental data or parameters. Thus, extending DDC methods to 2DOF control systems is in the developmental stage.

Unlike model-based design, the response of a closed-loop system after tuning the control parameters in the DDC method cannot be evaluated in advance. A data-driven approach does not always realize stable control parameters for a closed-loop system. Unstable control parameters may be generated when an inappropriate reference model is given for the structure or the order of the controllers [1], [2]. Various methods have been proposed to overcome these problems [1], [2], [31], [32], [33], [34]. The Estimated Response Iterative Tuning (ERIT) [31], [32], [33] uses one-shot input/output data to estimate the response after updating the feedforward control parameters of a 2DOF control system. The estimated response is subsequently used to tune the feedforward control parameters. However, the feedback characteristics such as the disturbance suppression performance cannot be enhanced because ERIT does not update the feedback controller.

Instability-detecting FRIT (ID-FRIT) [1], [2], [34] can estimate the response of a closed-loop system after updating the control parameters by offline computations of the finite impulse response of the closed-loop system using a fictitious reference signal [35] or a fictitious disturbance signal [36] calculated using one-shot input/output data. Furthermore, previous studies provided bounded-input/bounded-output (BIBO) stability for closed-loop systems. However, the controller structures treated in these methods [1], [2], [34] are one-degree-of-freedom (1DOF) control systems (feedback control systems), and these methods have yet to be extended to 2DOF control systems. Virtual Time-response-based Iterative Gain Evaluation and Redesign (V-Tiger) [37] is similar to [1], [2], and [34] in that the closed-loop systems are identified using input/output data, except the closed-loop identification is performed in the frequency domain. V-Tiger has been extended to 2DOF control systems [38], but both discrete-time Fourier transform and inverse discrete-time Fourier transform must be iteratively performed in nonlinear optimization calculations. Additionally, input/output data must be obtained up to the steady state.

In this study, we propose a direct data-driven method to enhance the tracking and disturbance suppression performance of a 2DOF control system using an estimation approach of the closed-loop output and control input. The proposed approach is based on the ID-FRIT framework, which provides an input/output estimation of the controlled object and the closed-loop BIBO stability after updating the feedback controller parameters without controller implementation. In addition, the proposed method generates unique optimal parameters, which are independent of the initial parameters.

Next, we describe the tuning scheme. The feedforward and feedback control parameters are tuned separately. First, the feedback control parameters are tuned to enhance the disturbance suppression performance. The target sensitivity function is given as an indicator of the disturbance suppression performance. The objective function is derived using a sensitivity function (finite impulse response) identified in the time domain. The input and output are fictitious disturbance signals, which are a function of the feedback control parameters, and the controlled-object input, respectively. Here, the objective function retains the pole information of the closed-loop system, and similar to ID-FRIT, the stability of the closed-loop system can be considered. Second, the feedforward control parameters are tuned to enhance the tracking performance. The target closed-loop transfer function is given as an indicator of the tracking performance. We derive an objective function using a transfer function (finite impulse response) identified in the time domain. The input and output are fictitious disturbance signals, which are fixed with the updated feedback control parameters, and the controlled-object output, respectively. Using the resultant finite impulse response, the response and control input after updating the control parameters can be estimated by an offline computation.

The rest of this paper is arranged as follows. First, we describe the problem setting and formulation. Second, we introduce the proposed method for tuning parameters in the feedback and feedforward controllers and explain how to prevent overfitting in the feedforward control parameter tuning and denoising method. Third, we validate the effectiveness of the proposed method via simulations and experiments. Finally, the conclusions of this paper are discussed.

[Notation] Let $x(k)$ be the time series signal x at step k. When the input time series signal $u(k)$ is applied to the single-input/single-output (SISO) LTI system $h(k)$, the response time series signal is given as $y(k) = h(k) * u(k)$. Here, the symbol $*$ denotes convolution. In the z-domain, the relationship between the input and output are described as $y(z) = H(z)u(z)$. $h(k)$ denotes the impulse response of

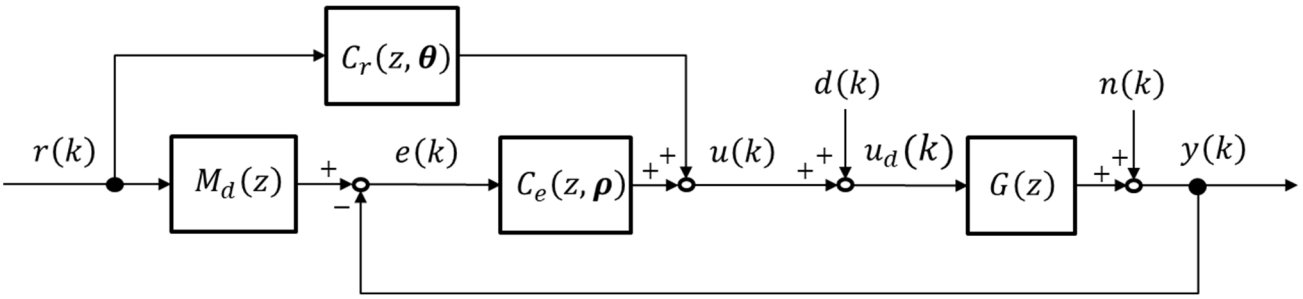

FIGURE 1. Two-degree-of-freedom control system.

$H(z)$. When the context is clear, $y(k) = H(z)\,u(k)$ is simply described instead of $y(k) = h(k) * u(k)$.

II. PROBLEM FORMULATION

This study considers the direct tuning problem for the feedback and feedforward control parameters of a 2DOF control system using only one-shot initial experimental closed-loop data to enhance the tracking and disturbance suppression performances. Figure 1 shows a 2DOF control system, where $G(z)$ is the controlled object, which is an unknown LTI and SISO system. $r(k)$, $e(k)$, $u(k)$, $d(k)$, $u_d(k)$, $n(k)$, and $y(k)$ indicate the reference input (target value), tracking error, control input (manipulated variable), input disturbance, controlled-object input, measurement noise, and controlled-object output (controlled variable) at step k, respectively. $C_e(z,\boldsymbol{\rho})$ and $C_r(z,\boldsymbol{\theta})$ are the feedback and feedforward controllers parameterized by the tuning parameter vectors $\boldsymbol{\rho} = \left[\rho_1 \cdots \rho_{n_e+m_e+1}\right]^T$ and $\boldsymbol{\theta} = \left[\theta_1 \cdots \theta_{n_r+m_r+1}\right]^T$, respectively. For instance, $C_e(z,\boldsymbol{\rho})$ and $C_r(z,\boldsymbol{\theta})$ in the z-domain are described as

$$C_e(z,\boldsymbol{\rho}) = \frac{\rho_{n_e+m_e+1}z^{m_e} + \cdots + \rho_{n_e+2}z + \rho_{n_e+1}}{\rho_{n_e}z^{n_e} + \cdots + \rho_1 z + 1} \tag{1}$$

$$C_r(z,\boldsymbol{\theta}) = \frac{\theta_{n_r+m_r+1}z^{m_r} + \cdots + \theta_{n_r+2}z + \theta_{n_r+1}}{\theta_{n_r}z^{n_r} + \cdots + \theta_1 z + 1} \tag{2}$$

The 2DOF control parameters $\boldsymbol{\rho}$ and $\boldsymbol{\theta}$ in Figure 1 are tuned by calculating separate objective functions to satisfy the two target characteristics: the target sensitivity function $S_d(z)$, and the target closed-loop transfer function $M_d(z)$. $S_d(z)$ and $M_d(z)$ are given independently. $S_d(z)$ is a sensitivity function that indicates the user-defined target sensitivity characteristic $u_d^*(k) = S_d(z)\,d(k)$ when $d \neq 0$ and $r = 0$. Here, we aim to obtain control parameters that minimize the following objective functions

$$J_S(\boldsymbol{\rho}) = \frac{1}{N}\sum_{k=0}^{N-1}\{e_S(k,\boldsymbol{\rho})\}^2 \tag{3}$$

$$e_S(k,\boldsymbol{\rho}) = u_d(k,\boldsymbol{\rho}) - S_d(z)\,d(k) \tag{4}$$

$M_d(z)$ is a transfer function indicating the user-defined target response $y^*(k) = M_d(z)\,r(k)$ when $r \neq 0$ and $d = 0$. We aim to obtain control parameters to minimize the following objective functions

$$J_M(\boldsymbol{\theta},\boldsymbol{\rho}) = \frac{1}{N}\sum_{k=0}^{N-1}\{e_M(k,\boldsymbol{\theta},\boldsymbol{\rho})\}^2 \tag{5}$$

$$e_M(k,\boldsymbol{\theta},\boldsymbol{\rho}) = y(k,\boldsymbol{\theta},\boldsymbol{\rho}) - M_d(z)\,r(k) \tag{6}$$

This paper employs a data-driven approach to obtain the optimal parameters of the feedback and feedforward controllers without modeling the controlled object.

III. DATA-DRIVEN TUNING FOR 2DOF CONTROL SYSTEMS

We develop a direct tuning method for the 2DOF control parameters based on a data-driven estimation approach. The proposed method consists of two steps: (i) design of the feedback control parameters to enhance the disturbance suppression performance and (ii) design of the feedforward control parameters to enhance tracking performance. The estimation uses one-shot closed-loop experimental data obtained from the initial experiments.

For the 2DOF control system shown in Figure 1, consider a feedback controller $C_e\left(z,\boldsymbol{\rho}^{\mathbf{0}}\right)$ and a feedforward controller $C_r\left(z,\boldsymbol{\theta}^{\mathbf{0}}\right)$ with initial parameters $\boldsymbol{\rho}^{\mathbf{0}}$ and $\boldsymbol{\theta}^{\mathbf{0}}$. It is assumed that the initial feedback controller $C_e\left(z,\boldsymbol{\rho}^{\mathbf{0}}\right)$ stabilizes the closed-loop system. First, one-shot time-series input/output data $u_{ini}\left(k,\boldsymbol{\theta}^{\mathbf{0}},\boldsymbol{\rho}^{\mathbf{0}}\right)$ and $y_{ini}\left(k,\boldsymbol{\theta}^{\mathbf{0}},\boldsymbol{\rho}^{\mathbf{0}}\right)$ are obtained by an initial closed-loop experiment with $r \neq 0$ and $d = 0$.

A. FEEDBACK CONTROLLER TUNING FOR ENHANCED DISTURBANCE SUPPRESSION PERFORMANCE

Herein tuning the feedback controller parameters to enhance the disturbance suppression performance is detailed. First, the controlled-object input $u_d(k,\boldsymbol{\rho})$ when $d \neq 0$ and $r = 0$ is estimated using initial input/output data $u_{ini}(k)$ and $y_{ini}(k)$. The relation between the input disturbance $d(k)$ and the controlled-obeject input $u_d(k)$ is given as

$$u_d(k) = \frac{1}{1 + G(z)\,C_e(z,\boldsymbol{\rho})}d(k) \tag{7}$$

Because $G(z)$ is unknown, (7) cannot be calculated as written above. Therefore, we introduce a fictitious disturbance

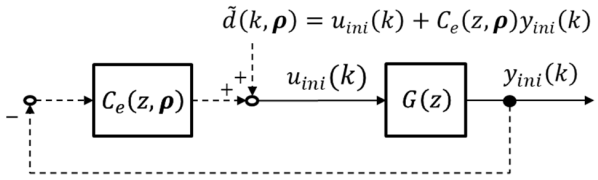

FIGURE 2. Fictitious feedback system.

signal [34], [36] defined as

$$\tilde{d}\left(k,\boldsymbol{\rho}\right) = u_{ini}\left(k\right) + C_e\left(z,\boldsymbol{\rho}\right) y_{ini}\left(k\right) \tag{8}$$

If $\tilde{d}\left(k,\boldsymbol{\rho}\right)$ is applied at the input of the controlled object as shown in Figure 2, the controlled-object input $u_d\left(k\right)$ and output $y\left(k\right)$ are fixed to the initial data $u_{ini}\left(k\right)$ and $y_{ini}\left(k\right)$ for an arbitrary stable controller $C_e\left(z,\boldsymbol{\rho}\right)$.

The transfer function from $\tilde{d}\left(k,\boldsymbol{\rho}\right)$ to $u_{ini}\left(k\right)$ is a sensitivity function $1\big/\left(1+G\left(z\right)C_e\left(z,\boldsymbol{\rho}\right)\right)$, which is given as

$$\tilde{S}\left(z,\boldsymbol{\rho}\right) = \frac{U_{ini}\left(z\right)}{\tilde{D}\left(z,\boldsymbol{\rho}\right)} = \frac{U_{ini}\left(z\right)}{U_{ini}\left(z\right) + C_e\left(z,\boldsymbol{\rho}\right) Y_{ini}\left(z\right)} \tag{9}$$

Although $G\left(z\right)$ is unknown, the sensitivity function with an arbitrary controller $C_e\left(z,\boldsymbol{\rho}\right)$ can be expressed from the initial data without directly using $G\left(z\right)$, as in (9). In the time domain, the relationship between $\tilde{d}\left(k,\boldsymbol{\rho}\right)$ and $u_{ini}\left(k\right)$ can be expressed using a convolutional representation as

$$u_{ini}\left(k\right) = \tilde{s}\left(k,\boldsymbol{\rho}\right) * \tilde{d}\left(k,\boldsymbol{\rho}\right) \tag{10}$$

where $\tilde{s}\left(k,\boldsymbol{\rho}\right)$ is the impulse response of the sensitivity function $\tilde{S}\left(z,\boldsymbol{\rho}\right)$. Equation (10) is calculated in the matrix form as

$$\boldsymbol{u_{ini}} = \tilde{\boldsymbol{D}}\left(\boldsymbol{\rho}\right)\cdot\tilde{\boldsymbol{s}}\left(\boldsymbol{\rho}\right) \tag{11}$$

$$\boldsymbol{u_{ini}} = \begin{bmatrix} u_{ini}\left(0\right) & \cdots & u_{ini}\left(N-1\right) \end{bmatrix}^T \tag{12}$$

$$\tilde{\boldsymbol{D}}\left(\boldsymbol{\rho}\right) = \begin{bmatrix} \tilde{d}\left(0,\boldsymbol{\rho}\right) & 0 & \cdots & 0 \\ \vdots & \tilde{d}\left(0,\boldsymbol{\rho}\right) & \ddots & 0 \\ \tilde{d}\left(N-2,\boldsymbol{\rho}\right) & \vdots & \ddots & 0 \\ \tilde{d}\left(N-1,\boldsymbol{\rho}\right) & \tilde{d}\left(N-2,\boldsymbol{\rho}\right) & \cdots & \tilde{d}\left(0,\boldsymbol{\rho}\right) \end{bmatrix} \tag{13}$$

$$\tilde{\boldsymbol{s}}\left(\boldsymbol{\rho}\right) = \begin{bmatrix} \tilde{s}\left(0,\boldsymbol{\rho}\right) & \cdots & \tilde{s}\left(N-1,\boldsymbol{\rho}\right) \end{bmatrix}^T \tag{14}$$

From (11), the impulse response $\tilde{\boldsymbol{s}}\left(\boldsymbol{\rho}\right)$ of the sensitivity function $\tilde{S}\left(z,\boldsymbol{\rho}\right)$ is the deconvolution of $\tilde{d}\left(k,\boldsymbol{\rho}\right)$ and $u_{ini}\left(k\right)$, or the solution of the linear equation $\tilde{\boldsymbol{D}}\left(\boldsymbol{\rho}\right)\cdot\tilde{\boldsymbol{s}}\left(\boldsymbol{\rho}\right) = \boldsymbol{u_{ini}}$ as in

$$\tilde{\boldsymbol{s}}\left(\boldsymbol{\rho}\right) = \left(\tilde{\boldsymbol{D}}\left(\boldsymbol{\rho}\right)^T\tilde{\boldsymbol{D}}\left(\boldsymbol{\rho}\right)\right)^{-1}\left(\tilde{\boldsymbol{D}}\left(\boldsymbol{\rho}\right)^T\boldsymbol{u_{ini}}\right) \tag{15}$$

Next, the estimated $u_{sd}\left(k,\boldsymbol{\rho}\right)$ when $d^{sup}\left(k\right)$ is applied to the sensitivity function $\tilde{S}\left(z,\boldsymbol{\rho}\right)$, which is the controlled-object input u_d when $d = d^{sup}$ and $r = 0$, is given by the convolution expression as

$$u_{sd}\left(k,\boldsymbol{\rho}\right) = \tilde{s}\left(k,\boldsymbol{\rho}\right) * d^{sup}\left(k\right) \tag{16}$$

where $d^{sup}\left(k\right)$ is the disturbance signal to be suppressed. The user can arbitrarily assign $d^{sup}\left(k\right)$. Equation (16) can be calculated in a matrix form similar to (11-14). The objective function is the sum of the squares error between $u_{sd}\left(k,\boldsymbol{\rho}\right)$ obtained here and the response of the target sensitivity function $u^*\left(k\right) = S_d\left(z\right)d^{sup}\left(k\right)$. Note that this objective function contains pole information of the closed-loop system. Hence, it is possible to consider the BIBO stability of the closed-loop system similar to ID-FRIT [1], [2].

$$\boldsymbol{\rho}^* = \arg\min_{\boldsymbol{\rho}} \widetilde{J}_S\left(\boldsymbol{\rho}\right) \tag{17}$$

$$\widetilde{J}_S\left(\boldsymbol{\rho}\right) = \frac{1}{N}\sum_{k=0}^{N-1}\left\{\varepsilon_S\left(k,\boldsymbol{\rho}\right)\right\}^2 \tag{18}$$

$$\varepsilon_S\left(k,\boldsymbol{\rho}\right) = u_{sd}\left(k,\boldsymbol{\rho}\right) - S_d\left(z\right)d^{sup}\left(k\right) \tag{19}$$

This optimization problem is solved using nonlinear optimization methods. We interpret the objective function using Parseval's theorem. As N approaches infinity, it is described as

$$\widetilde{J}_S\left(\boldsymbol{\rho}\right) = \frac{1}{2\pi}\int_{-\pi}^{\pi}\left|1 - \frac{S\left(e^{j\omega},\boldsymbol{\rho}\right)}{S_d\left(e^{j\omega}\right)}\right|^2\Phi_{u^*}d\omega \tag{20}$$

where Φ_{u^*} is the power spectral density of the response of target sensitivity function $u^*\left(k\right) = S_d\left(z\right)d^{sup}\left(k\right)$. Here, the relative error between the target sensitivity function S_d and the sensitivity function $S\left(\boldsymbol{\rho}\right)$ is evaluated for an arbitrary $C_e\left(z,\boldsymbol{\rho}\right)$. In noiseless situations, the objective function shown in (18) is equivalent to the evaluation function shown in (3) when $d^{sup} = d$, and optimality is ensured. However, the identification of the sensitivity function shown in (15) may cause errors under noisy conditions, resulting in non-optimal values. To avoid this, the filtering method shown in section III-D is used. When given an appropriate S_d, the model matching shown in equation (3) is achieved, enhancing the disturbance suppression performance. Considering the persistent excitation condition, initial experimental data, which sufficiently excites the system characteristics, should be obtained to identify the sensitivity function accurately. For this reason, an open-loop experiment using random input signals is desirable. Because this is difficult for real systems, herein the closed-loop (step) response data is used. A satisfactory performance is obtained in this paper.

The optimal parameter $\boldsymbol{\rho}^*$ obtained by the proposed method is unique. That is, unlike VIMT [29] and [30], the optimal parameter to minimize the objective function is independent of the initial control parameters. Furthermore, unlike VRFT-2DOF [28], there is no need to calculate the power spectral density of the initial data or to prepare the prefilter. Herein, the covariance matrix adaptation evolution strategy (CMA-ES) [39] is used as a nonlinear optimization method. Its effectiveness has been confirmed elsewhere [2], [40].

B. FEEDFORWARD CONTROLLER TUNING FOR ENHANCED TRACKING PERFORMANCE

1) MAIN

The feedforward control parameters are tuned to enhance the tracking performance. First, initial input/output data, $u_{ini}\left(k\right)$

and $y_{ini}(k)$, and the updated feedback controller $C_e(z, \boldsymbol{\rho}^*)$ are used to estimate the output $y(k, \boldsymbol{\theta}, \boldsymbol{\rho}^*) = y_{tr}(k, \boldsymbol{\theta}, \boldsymbol{\rho}^*)$ when $r \neq 0$ and $d = 0$. Here, $y_{tr}(k, \boldsymbol{\theta}, \boldsymbol{\rho}^*)$ is expressed as

$$y_{tr}(k, \boldsymbol{\theta}, \boldsymbol{\rho}^*) = \frac{G(z)\left(C_r(z, \boldsymbol{\theta}) + C_e(z, \boldsymbol{\rho}^*) M_d(z)\right)}{1 + G(z) C_e(z, \boldsymbol{\rho}^*)} r(k) \quad (21)$$

$y_{tr}(k, \boldsymbol{\theta}, \boldsymbol{\rho}^*)$ can also be expressed as

$$y_{tr}(k, \boldsymbol{\theta}, \boldsymbol{\rho}^*) = \left(C_r(z, \boldsymbol{\theta}) + C_e(z, \boldsymbol{\rho}^*) M_d(z)\right) y_{wr}(k, \boldsymbol{\rho}^*) \quad (22)$$

$$y_{wr}(k, \boldsymbol{\rho}^*) = W(k, \boldsymbol{\rho}^*) r(k) \quad (23)$$

$$W(z, \boldsymbol{\rho}^*) = \frac{G(z)}{1 + G(z) C_e(z, \boldsymbol{\rho}^*)} \quad (24)$$

In this paper, we initially calculate $W(k, \boldsymbol{\rho}^*)$. Then, $y_{wr}(k, \boldsymbol{\rho}^*)$ is obtained by (23). Finally, the response $y_{tr}(k, \boldsymbol{\theta}, \boldsymbol{\rho}^*)$ when $r \neq 0$ and $d = 0$ is calculated using (22) for an arbitrary feedforward controller $C_r(z, \boldsymbol{\theta})$.

Consider a one-shot fictitious disturbance signal $\tilde{d}(k, \boldsymbol{\rho}^*)$ in the updated feedback controller $C_e(z, \boldsymbol{\rho}^*)$. The transfer function from $\tilde{d}(k, \boldsymbol{\rho}^*)$ to $y_{ini}(k)$ is $W(z, \boldsymbol{\rho}^*)$.

$$\tilde{W}(z, \boldsymbol{\rho}^*) = \frac{Y_{ini}(z)}{\tilde{D}(z, \boldsymbol{\rho}^*)} = \frac{Y_{ini}(z)}{U_{ini}(z) + C_e(z, \boldsymbol{\rho}^*) Y_{ini}(z)} \quad (25)$$

In the time domain, the relationship between $\tilde{d}(k, \boldsymbol{\rho}^*)$ and $y_{ini}(k)$ can be expressed using a convolutional representation as

$$y_{ini}(k) = \tilde{w}^*(k, \boldsymbol{\rho}^*) * \tilde{d}(k, \boldsymbol{\rho}^*) \quad (26)$$

where $\tilde{w}^*(k, \boldsymbol{\rho}^*)$ denotes the impulse response of the transfer function $\tilde{W}(z, \boldsymbol{\rho}^*)$. Similar to (11-14), (26) can be calculated in the matrix form. The impulse response $\tilde{w}^*(\boldsymbol{\rho}^*)$ of the transfer function $\tilde{W}(z, \boldsymbol{\rho}^*)$ is the deconvolution of $\tilde{d}(k, \boldsymbol{\rho})$ and $y_{ini}(k)$, or the solution of the linear equation $\tilde{D}(\boldsymbol{\rho}^*) \cdot \tilde{w}^*(\boldsymbol{\rho}^*) = \boldsymbol{y_{ini}}$ as

$$\tilde{\boldsymbol{w}}^*(\boldsymbol{\rho}^*) = \left(\tilde{\boldsymbol{D}}(\boldsymbol{\rho}^*)^{\boldsymbol{T}} \tilde{\boldsymbol{D}}(\boldsymbol{\rho}^*)\right)^{-1} \left(\tilde{\boldsymbol{D}}(\boldsymbol{\rho}^*)^{\boldsymbol{T}} \boldsymbol{y_{ini}}\right) \quad (27)$$

$$\boldsymbol{y_{ini}} = \left[\, y_{ini}(0) \quad \cdots \quad y_{ini}(N-1) \,\right]^T \quad (28)$$

where $\tilde{\boldsymbol{D}}(\boldsymbol{\rho}^*)$ is the matrix with $\boldsymbol{\rho} = \boldsymbol{\rho}^*$ in (13). Next, $y_{wr}(k, \boldsymbol{\rho}^*)$ is given by the convolution expression as

$$y_{wr}(k, \boldsymbol{\rho}^*) = \tilde{w}^*(k, \boldsymbol{\rho}^*) * r(k) \quad (29)$$

Similar to (11-14), (29) can be calculated in the matrix form. Using the obtained $y_{wr}(k, \boldsymbol{\rho}^*)$, the estimated controlled-object output $y_{tr}(k, \boldsymbol{\theta}, \boldsymbol{\rho}^*)$ for an arbitrary $C_r(z, \boldsymbol{\theta})$ when $r \neq 0$ and $d = 0$ can be calculated using (22). The control input $u_{tr}(k, \boldsymbol{\theta}, \boldsymbol{\rho}^*)$ can also be calculated as

$$u_{tr}(k, \boldsymbol{\theta}, \boldsymbol{\rho}^*) = \left(C_r(z, \boldsymbol{\theta}) + C_e(z, \boldsymbol{\rho}^*) M_d(z)\right) r(k) - C_e(z, \boldsymbol{\rho}^*) y_{tr}(k, \boldsymbol{\theta}, \boldsymbol{\rho}^*) \quad (30)$$

The objective function is the sum of the squares error between $y_{tr}(k, \boldsymbol{\theta}, \boldsymbol{\rho}^*)$ obtained here and the target response $y^*(k) = M_d(z) r(k)$.

$$\boldsymbol{\theta}^* = \arg\min_{\boldsymbol{\theta}} \widetilde{J_M}(\boldsymbol{\theta}) \quad (31)$$

$$\widetilde{J_M}(\boldsymbol{\theta}) = \frac{1}{N} \sum_{k=0}^{N-1} \{\varepsilon_M(k, \boldsymbol{\theta})\}^2 \quad (32)$$

$$\varepsilon_M(k, \boldsymbol{\theta}) = y_{tr}(k, \boldsymbol{\theta}, \boldsymbol{\rho}^*) - M_d(z) r(k) \quad (33)$$

Finally, the optimal feedforward controller parameter $\boldsymbol{\theta}^*$ to minimize the objective function shown in (32) is obtained. The objective function shown in (32) is equivalent to (5) under noiseless conditions, and optimality is ensured.

We interpret the objective function using Parseval's theorem. As N approaches infinity,

$$\widetilde{J_M}(\boldsymbol{\theta}) = \frac{1}{2\pi} \int_{-\pi}^{\pi} \left| 1 - \frac{T(e^{j\omega}, \boldsymbol{\theta}, \boldsymbol{\rho}^*)}{M_d(e^{j\omega})} \right|^2 \Phi_{y^*} d\omega \quad (34)$$

where Φ_{y^*} is the power spectral density of the target response $y^*(k) = M_d(z) r(k)$. The relative error between the target closed-loop transfer function M_d and the closed-loop transfer function $T(z, \boldsymbol{\theta}, \boldsymbol{\rho}^*)$ using an arbitrary $C_r(z, \boldsymbol{\theta})$ is evaluated. Unlike VIMT [29], [30], the optimal parameter to minimize the objective function of the proposed method is independent of the initial control parameters. Unlike in VRFT-2DOF [28], neither calculation of the power spectral density of the initial data nor preparation of a prefilter is required. The optimal feedforward control parameter $\boldsymbol{\theta}^*$ can be obtained by a nonlinear optimization. If $C_r(z, \boldsymbol{\theta})$ is parameterized by a linear function of $\boldsymbol{\theta}$ as shown below, the least squares method can be used.

$$C_r(z, \boldsymbol{\theta}) = \boldsymbol{\theta}^T \boldsymbol{\beta}(z) \quad (35)$$

$$\boldsymbol{\beta}(z) = \left[\, \beta_1(z) \quad \beta_2(z) \quad \cdots \quad \beta_n(z) \,\right]^T \quad (36)$$

The number of tuning feedforward control parameters is assumed to be n. In the case of (35), the optimal parameter $\boldsymbol{\theta}^*$ is obtained as

$$\boldsymbol{\theta}^* = \left(\boldsymbol{\Theta}^T \boldsymbol{\Theta}\right)^{-1} \left(\boldsymbol{\Theta}^T \boldsymbol{y_s}\right) \quad (37)$$

$$\boldsymbol{\Theta} = \begin{bmatrix} \beta_1(z) y_{wr}(1) & \cdots & \beta_n(z) y_{wr}(1) \\ \vdots & \ddots & \vdots \\ \beta_1(z) y_{wr}(N) & \cdots & \beta_n(z) y_{wr}(N) \end{bmatrix} \quad (38)$$

$$\boldsymbol{y_s} = \left[\, y_s(0) \quad \cdots \quad y_s(N-1) \,\right]^T \quad (39)$$

$$y_s(k) = M_d(z) \left(r(k) - C_e(z, \boldsymbol{\rho}^*) y_{wr}(k, \boldsymbol{\rho}^*)\right) \quad (40)$$

When the initial data obtained under noisy conditions is used, a non-optimal value, which minimizes the objective function (5), may be calculated. To reduce this effect, the instrumental variable method may be considered, but the variance may increase. Hence, this paper uses Ridge regression as described below.

2) PREVENTING OVERFITTING IN FEEDFORWARD CONTROLLER TUNING

Here, it is assumed that a finite impulse response (FIR) filter with $\beta_i(z) = z^{1-i}$ is used for (36). Considering model matching between the target closed-loop transfer function $M_d(z)$ and the closed-loop transfer function from $r(k)$ to $y(k)$ shown in Figure 1, the ideal model for the feedforward controller is given as $C_r^*(z) = M_d(z) G^{-1}(z)$. Thus, a finite impulse response of $M_d(z) G^{-1}(z)$ is identified. However, overfitting may cause the identified FIR filter coefficients (tuning parameters) to become excessive. If the FIR filter coefficients in the feedforward controller are too large, the control input may also be too large. In real situations, hardware limitations prevent applying the control input. Consequently, the following objective function constrains the tuning parameters

$$\widetilde{J_M^R}(\boldsymbol{\theta}) = \frac{1}{N}\left(\sum_{k=0}^{N-1}\{\varepsilon_M(k,\boldsymbol{\theta})\}^2 + k_R\sum_{i=1}^{n}\theta_i^2\right) \tag{41}$$

The minimization problem in (41) corresponds to a ridge regression [41], [42]. Instead of (37), the feedforward control parameters are calculated using the following equation

$$\boldsymbol{\theta}_{\boldsymbol{R}}^* = \left(\boldsymbol{\Theta}^T\boldsymbol{\Theta} + k_R\boldsymbol{I_n}\right)^{-1}\left(\boldsymbol{\Theta}^T\boldsymbol{y_s}\right) \tag{42}$$

where $k_R \geq 0$ and $\boldsymbol{I_n}$ is an $n \times n$ unit matrix. Equation (42) can be used to prevent overfitting of the tuning parameters in the feedforward controller. Therefore, selecting an appropriate value for k_R can prevent excessive tuning parameters (FIR filter coefficients). The calculated tuning parameters depend on k_R, and the response also shows different results. However, a re-experiment to determine the appropriate k_R is unnecessary since the control input and response after parameter tuning can be computed offline in advance when using arbitrary k_R by (43) and (45).

C. ESTIMATING THE RESPONSE AND CONTROL INPUT AFTER THE PARAMETER UPDATE

In the 2DOF control system shown in Figure 1, the response $\hat{y}(k, \boldsymbol{\theta}^*, \boldsymbol{\rho^*})$ when $r \neq 0$ and $d \neq 0$ after updating the feedback and feedforward controller to the tuned parameters $\boldsymbol{\rho^*}$ and $\boldsymbol{\theta}^*$ can be estimated as

$$\hat{y}(k, \boldsymbol{\theta}^*, \boldsymbol{\rho^*}) = y_{tr}(k, \boldsymbol{\theta}^*, \boldsymbol{\rho^*}) + y_{w\hat{d}}(k, \boldsymbol{\rho^*}) \tag{43}$$

The first term $y_{tr}(k, \boldsymbol{\theta}^*, \boldsymbol{\rho^*})$ is a component of the reference signal $r(k)$ and is calculated by (22) with $\boldsymbol{\theta}$ fixed to the update parameter $\boldsymbol{\theta}^*$. The second term $y_{w\hat{d}}(k, \boldsymbol{\rho^*})$ is a component of the input disturbance $d(k)$ and is expressed in the time domain as

$$y_{w\hat{d}}(k, \boldsymbol{\rho^*}) = \tilde{w}^*(k, \boldsymbol{\rho^*}) * \hat{d}(k) \tag{44}$$

In other words, it is the disturbance response showing $y_{w\hat{d}}(k, \boldsymbol{\rho^*}) = \left(G(z)/1 + G(z) C_e(z, \boldsymbol{\rho^*})\right)\hat{d}(k)$. Here, $\hat{d}(k)$ is the input disturbance, which is the input disturbance assumed by the user (usually, the disturbance is unknown). It can be distinguished from $d^{sup}(k)$ in (16) and given independently of each other. Similar to (11-14), (44) can be calculated in the matrix form. The control input $\hat{u}(k, \boldsymbol{\theta}^*, \boldsymbol{\rho^*})$ after updating can be estimated as

$$\hat{u}(k, \boldsymbol{\theta}^*, \boldsymbol{\rho^*}) = u_{tr}(k, \boldsymbol{\theta}^*, \boldsymbol{\rho^*}) + u_{w\hat{d}}(k, \boldsymbol{\rho^*}) \tag{45}$$

The first term $u_{tr}(k, \boldsymbol{\theta}^*, \boldsymbol{\rho^*})$ is a component of the reference signal $r(k)$ and is calculated by (30) with $\boldsymbol{\theta}$ fixed to the update parameter $\boldsymbol{\theta}^*$. The second term $u_{w\hat{d}}(k, \boldsymbol{\rho^*})$ is a component of the input disturbance $d(k)$ and can be expressed using $y_{w\hat{d}}(k, \boldsymbol{\rho^*})$ as

$$u_{w\hat{d}}(k, \boldsymbol{\rho^*}) = -C_e(z, \boldsymbol{\rho^*})\, y_{w\hat{d}}(k, \boldsymbol{\rho^*}) \tag{46}$$

Thus, the initial input/output data $u_{ini}(k)$, $y_{ini}(k)$ and offline computations without a re-experiment can estimate the response and control input after parameter updating. This is an advantage compared to FRIT-2DOF [26] and VRFT-2DOF [28] as it can evaluate the effects of parameter tuning using the computer in advance, enabling efficient control system design.

The proposed method is superior to previously proposed methods. Although ERIT [31], [32], [33] deals with 2DOF control systems and estimates the response and control input after updating only the feedforward controller, the feedback controller is assumed to be invariant. By contrast, the proposed method does not assume invariance. In addition, the control structures treated in ID-FRIT [1], [2] and the method in [34] are 1DOF control systems (feedback control systems), whereas the proposed method deals with 2DOF control systems.

D. HANDLING NOISE

In a real environment, the obtained initial input/output data contains noise. Under noisy conditions, the initial input/output data $u_{ini}(k)$ and $y_{ini}(k)$ can be expressed as

$$\begin{aligned} u_{ini}(k) = {} & \frac{C_r(z, \boldsymbol{\theta^0}) + C_e(z, \boldsymbol{\rho^0}) M_d(z)}{1 + G(z) C_e(z, \boldsymbol{\rho^0})} r(k) \\ & - \frac{C_e(z, \boldsymbol{\rho^0})}{1 + G(z) C_e(z, \boldsymbol{\rho^0})} n(k) \end{aligned} \tag{47}$$

$$\begin{aligned} y_{ini}(k) = {} & \frac{G(z)\left(C_r(z, \boldsymbol{\theta^0}) + C_e(z, \boldsymbol{\rho^0}) M_d(z)\right)}{1 + G(z) C_e(z, \boldsymbol{\rho^0})} r(k) \\ & + \frac{1}{1 + G(z) C_e(z, \boldsymbol{\rho^0})} n(k) \end{aligned} \tag{48}$$

where the input disturbance $d(k)$ is assumed to be zero. The $r(k)$ component of $y_{ini}(k)$ given by the first term in (48) has a low-pass property and attenuates in the high-frequency range. The $n(k)$ component of $y_{ini}(k)$ given by the second term in (48) is a sensitivity function, which has a high-pass characteristic. Therefore, the signal-to-noise (S/N) ratio of $y_{ini}(k)$ deteriorates in the high-frequency range. Furthermore, if $r(k)$ and $n(k)$ are assumed to be the step signal and white noise,

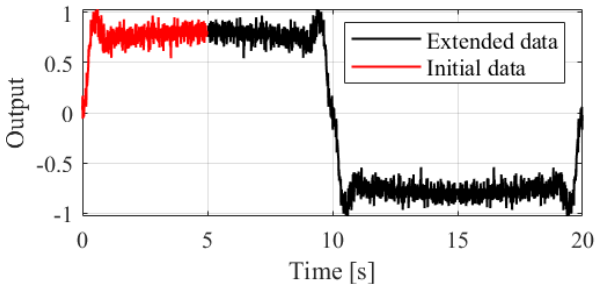

FIGURE 3. Extension of the step response data $y_{ini}(k)$.

respectively, the S/N of $u_{ini}(k)$ should also degrade in the high-frequency range [1], [43].

To overcome this, high-frequency noise is eliminated from the initial data. The discrete Fourier transform (DFT) is used to denoise the initial data in the frequency domain. First, we consider the output data. Suppose that the step response data with data length N is obtained as the output data. If the DFT for $y_{ini}(k)$ is performed, $y_{ini}(k)$ is given as

$$Y(j\omega_k) = \mathcal{F}[y_{ini}(k)] \tag{49}$$

where $\mathcal{F}[\cdot]$ denotes the DFT and $\mathcal{F}^{-1}[\cdot]$ denotes its inverse transform. $j\omega_k$ is the angular frequency corresponding to k. The high-frequency component of $Y(j\omega_k)$ is attenuated as

$$\left\{Y_f(j\omega_k)\right\}_{k=k_l,\cdots,k_{Nyq},\cdots k_h} = \{\beta Y(j\omega_k)\}_{k=k_l,\cdots,k_{Nyq},\cdots k_h} \tag{50}$$

where $\beta < 1$ is the attenuation rate and $\omega_{k_{Nyq}}$ is the Nyquist frequency. Since the DFT generates complex conjugate pairs that are symmetric with respect to the Nyquist frequency, each complex conjugate pair must be multiplied by the same attenuation rate for its inverse transform to become a real number. Finally, $Y_f(j\omega_k)$ is inversely transformed to obtain the output data $y_f(k)$ without high-frequency noise.

$$y_f(k) = \mathcal{F}^{-1}\left[Y_f(j\omega_k)\right] \tag{51}$$

To apply a Fourier transform, the signal must be periodic. However, step response data are generally discontinuous between the start and end points. In this case, $y_f(k)$ becomes a signal, which is connected at the start and end points and has components that are not included in the original data. Here, we extend the response data $y_{ini}(k)$ to $y_b(k)$ using the following equation, as shown in Figure 3.

$$\begin{aligned} y_b(k) = \{&y_a(0), y_a(1), \cdots, y_a(2N-1), \\ &-y_a(2N-1), \cdots, -y_a(1), -y_a(0)\} \end{aligned} \tag{52}$$

$$\begin{aligned} y_a(k) = \{&y_{ini}(0), y_{ini}(1), \cdots, y_{ini}(N-1), \\ &y_{ini}(N-1), \cdots, y_{ini}(1), y_{ini}(0)\} \end{aligned} \tag{53}$$

The extended data $y_b(k)$ is odd function data with a data length of $4N$. Substituting $y_b(k)$ for $y_{ini}(k)$ in (49) gives $y'_f(k)$ with the high-frequency components eliminated by the calculation procedures (50) and (51). $y'_f(k)$ has a data length of $4N$; thus, $y^*_f(k)$ with $k = 0, \cdots, N-1$ is expressed as

$$\left\{y^*_f(k)\right\} = \left\{y'_f(k)\right\}_{k=0,\cdots,N-1} \tag{54}$$

The expanded data $y_b(k)$ has the same start and end points, preventing discontinuity. The odd function can be expanded to the sum of the sine waves. Since sine waves are origin-symmetric signals, the initial condition $y(0) = 0$ of the original data can be considered even after the high-frequency components are attenuated. Using the output data $y^*_f(k)$ with the noise removed, the denoised control input data $u^*_f(k)$ is obtained as

$$\begin{aligned} u^*_f(k) = &\left(C_r\left(z, \boldsymbol{\theta}^{\mathbf{0}}\right) + C_e\left(z, \boldsymbol{\rho}^{\mathbf{0}}\right) M_d(z)\right) r(k) \\ &- C_e\left(z, \boldsymbol{\rho}^{\mathbf{0}}\right) y^*_f(k) \end{aligned} \tag{55}$$

IV. SIMULATION VALIDATION

Numerical simulations verified the proposed method.

A. SIMULATION CONDITIONS

The target closed-loop transfer function $M_d(z)$ is the second-order system without overshooting [1], [19], [26], which is given as

$$M_d(z) = z(M_d(s)) \tag{56}$$

$$M_d(s) = \frac{1}{(\tau_M s + 1)^2} \tag{57}$$

where s is the Laplace operator and $z(\cdot)$ is the operator to convert from the continuous time domain to the discrete time domain. τ_M is a parameter related to the responsiveness. Next the target sensitivity function $S_d(z)$ is the first-order high-pass filter given as

$$S_d(z) = z(S_d(s)) \tag{58}$$

$$S_d(s) = \frac{\tau_S s}{\tau_S s + 1} \tag{59}$$

where τ_S is a parameter (time constant) related to the disturbance suppressibility. Here, the high-pass filter is used to suppress the input disturbance $d(k)$, which is assumed to have a dominant low-frequency component, especially for the constant value disturbance. The feedback controller $C_e(z, \boldsymbol{\rho})$ and the feedforward controller $C_r(z, \boldsymbol{\theta})$ are a PID controller and an FIR filter type controller, respectively, which are expressed as

$$C_e(z, \boldsymbol{\rho}) = \boldsymbol{\rho}^T \boldsymbol{\alpha}(z) \tag{60}$$

$$\boldsymbol{\rho}^T = \begin{bmatrix} K_p & K_i & K_d \end{bmatrix} \tag{61}$$

$$\boldsymbol{\alpha}(z) = \begin{bmatrix} 1 & \dfrac{T_s}{1-z^{-1}} & \dfrac{1}{\tau_f + \frac{T_s}{1-z^{-1}}} \end{bmatrix}^T \tag{62}$$

$$C_r(z, \boldsymbol{\theta}) = \boldsymbol{\theta}^T \boldsymbol{\beta}(z) \tag{63}$$

$$\boldsymbol{\theta}^T = \begin{bmatrix} k_1 & k_2 & \cdots & k_{10} \end{bmatrix} \tag{64}$$

$$\boldsymbol{\beta}(z) = \begin{bmatrix} 1 & z^{-1} & \cdots & z^{-10} \end{bmatrix}^T \tag{65}$$

where τ_f is the filter time constant for the approximate derivative. In the simulation, $\tau_f = 0.1$. T_s is the sampling time. The controlled object $G(z)$ is a spring-mass system, which is used in many industries [1], and is given as

$$G(z) = z(G(s)) \tag{66}$$

$$G(s) = \frac{1}{(0.01s+1)\left(0.1s^2+0.5s+5\right)} e^{-Ls} \tag{67}$$

where L is the dead time.

The responsively parameter of the target closed-loop transfer function $M_d(z)$ is $\tau_M = 0.05$, and the time constant of the target sensitivity function $S_d(z)$ is $\tau_S = 0.2$. The dead time is $L = 0$. The sampling time T_s is set to 10 ms, and the initial input/output data are obtained from 0.0 to 5.0 s. Table 1 shows the initial PID gain $\boldsymbol{\rho}^{\mathbf{0}}$ of the feedback controller. The initial filter coefficient $\boldsymbol{\theta}^{\mathbf{0}}$ of the feedforward controller is given as

$$\theta_i^0 = k_i^0 = \frac{1}{81}(10-i)^2 \tag{68}$$

In Table 1, the root-mean-square of $\boldsymbol{\theta}$ ($RMS[\boldsymbol{\theta}]$) is shown, where $RMS[\boldsymbol{\theta}]$ is defined as

$$RMS[\boldsymbol{\theta}] = \sqrt{\frac{1}{n}\sum_{i=1}^{n}\theta_i^2} = \sqrt{\frac{1}{10}\sum_{i=1}^{10}k_i^2} \tag{69}$$

B. SIMULATION RESULTS AND DISCUSSION

The effectiveness of the proposed method was verified for two cases. Case 1 is the ideal condition, which is free from noise. That is, the variance value of white noise $n(k)$ in Figure 1 is zero. Case 2 is the noisy condition. The simulation for Case 2 set the variance value of white noise $n(k)$ to 0.005 and applied the denoising method described in section III-D.

Table 1 shows the values in Case 1 before and after tuning for the feedback control parameters, root-mean-square of the feedforward control parameters, and objective function. $d^{sup}(k)$ in the feedback control parameter tuning is a step signal with $d^{sup}(k \geq 0) = 1.0$ to suppress a constant value disturbance. All of the objective function values decrease significantly after tuning compared to before tuning.

Figure 4 plots the value of the objective function $\widetilde{J}_S$ for the number of CMA-ES iterations in the feedback control parameters tuning. The values converged appropriately.

Figure 5 shows the response and control input estimation results (from 0.00 to 2.50 s) after tuning as calculated by (43) and (45) with different ridge regression parameters k_R described in section III-B. Here, the step reference input $r(k \geq 0) = 1.0$ and the assumed input disturbance $\hat{d}(k) = 0.0$ are used. The ridge regression parameters in the feedforward control parameter tuning are compared for $k_R = 0$, 10^{-6}, and 10^{-4}.

The norm of the tuning parameter of the feedforward controller is smaller when ridge regression is used (Table 1). However, the estimated responses are similar for all conditions (Figure 5(a)), suggesting overfitting occurs, especially when $k_R = 0$, where ridge regression is not used. Employing ridge regression can prevent the control input from becoming too large (Figure 5(b)). Below, the effects of the tuning parameters at $k_R = 10^{-4}$ are discussed.

TABLE 1. Control parameters and the value of the objective function in Case 1: Ideal condition.

Symbol		Before tuning	After tuning
Feedback Controller	K_p	+0.2000	+2.0975
	K_i	+0.5000	+24.3077
	K_d	+0.0100	+0.5121
Feedforward Controller	RMS[$\boldsymbol{\theta}$]	0.4834	727.199 ($k_R = 0$) 41.739 ($k_R = 10^{-6}$) 14.854 ($k_R = 10^{-4}$)
Objective function	$\widetilde{J}_S(\boldsymbol{\rho})$	0.5463	1.0768×10^{-4}
	$\widetilde{J}_M(\boldsymbol{\theta})$	0.05757	2.458×10^{-4} ($k_R = 0$) 3.298×10^{-4} ($k_R = 10^{-6}$) 4.984×10^{-4} ($k_R = 10^{-4}$)
	J_S	0.5095	1.0769×10^{-4}
	J_M	0.05757	4.984×10^{-4}

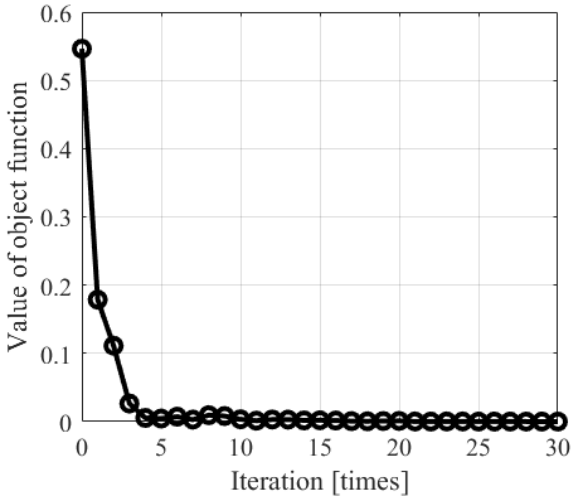

FIGURE 4. Variation of the objective function value with respect to the number of iterations in the optimization.

First, a simulation for Case 1 is conducted to evaluate the tracking performance after parameter tuning using input disturbance $d(k) = 0$ and step-reference input $r(k) = 1.0$. Figures 6(a)–(d) show the simulation results for the output, control input, feedforward control input, and feedback control input, respectively. Prior to tuning, the tracking performance is poor. Tuning enhances the performance. The proposed method (43) and (45) can accurately estimate the response and control input after tuning (Figures 6(a) and (b), blue lines).

Second, a simulation for Case 1 is conducted to evaluate the disturbance suppression performance using the reference input $r(k) = 0.0$ and input disturbance $d(k) = 1.0$ as a step signal (step start time is 0.50 s). Figures 7(a)–(c) show the simulation results for the output, control input, and input

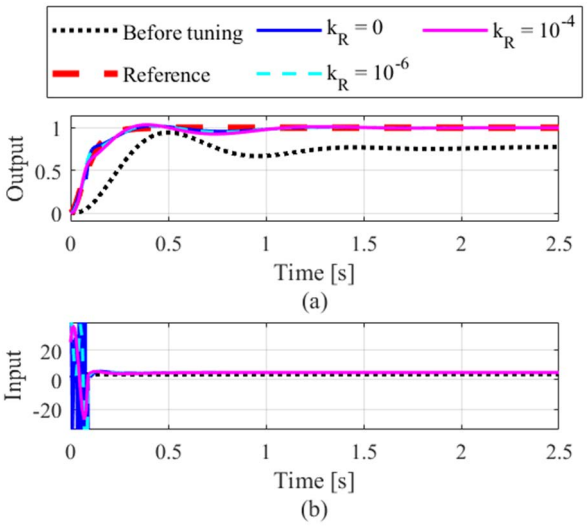

FIGURE 5. Estimated input and output time series data with different k_R values for ridge regression in Case 1. (a) Output, (b) input.

disturbance, respectively. Similar to the tracking performance results, the disturbance suppression performance for step disturbance prior to tuning is poor, but it is enhanced after tuning. The proposed method (43) and (45) calculated the estimated response and control inputs in advance (Figures 7(a) and (b), blue lines). Generally, the input disturbance $d\,(k)$ is unknown. Herein, an assumed input disturbance $\hat{d}\,(k) = 1.0$ was used to evaluate the estimation accuracy of (43) and (45). The proposed method (43) and (45) can accurately estimate the response and control input after tuning.

Next, the simulation results under noisy conditions (Case 2) were considered. Figure 8 (black) shows the initial input/output data from 0.0 to 5.0 s. These input/output data were denoised using the method described in section III-D. The cutoff frequency ω_{kl} was selected by evaluating the initial tracking error $e_{ini}\,(k) = y_{ini}\,(k) - M_d\,(z)\,r\,(k)$ in the frequency domain [31]. Figure 9 shows the DFT results for $e_{ini}\,(k)$, where the horizontal and vertical axis indicate the frequency and $20\log_{10}|e_{ini}\,(j\omega)|$, respectively. The cutoff frequency ω_{kl} is 6.0 Hz, judging that the noise is dominant from 6.0 Hz. The attenuation rate β in (59) was set to 0.0001. Figure 7 shows the denoised input/output data, which was used for parameter tuning.

Table 2 shows the values before and after tuning in Case 2 for the feedback control parameters, root-mean-square of the feedforward control parameters, and objective function. Similar to Case 1, $d^{sup}\,(k)$ in the feedback control parameter tuning is a step signal with $d^{sup}\,(k \geq 0) = 1.0$.

Figure 10 shows the response and control input estimation results (from 0.00 to 2.50 s) after tuning as calculated by (43) and (45) with the different ridge regression parameters k_R described in section III-B. Here, the step reference input $r\,(k \geq 0) = 1.0$ and the assumed input disturbance $\hat{d}\,(k) = 0.0$ were used. $k_R = 0, 10^{-6}$, and 10^{-4} were compared to those in Case 1. The estimated responses are similar when

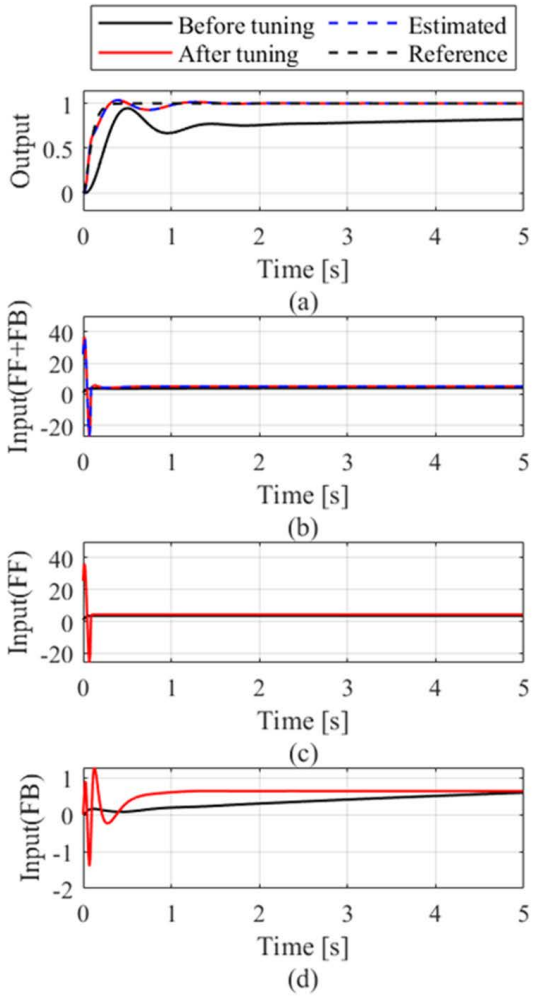

FIGURE 6. Input and output time series data of the set-point response simulation for Case1. (a) Output, (b) control input, (c) feedforward control input, (d) feedback control input.

$k_R > 0$. However, the estimated control input can be prevented from becoming too large by selecting an appropriate value for k_R. Based on these results, below the effects of the tuning parameters at $k_R = 10^{-4}$ are verified.

First, a simulation for Case 2 was conducted to evaluate the tracking performance after parameter tuning using an input disturbance $d\,(k) = 0$ and step reference input $r\,(k) = 1.0$. Figures 11(a)–(d) show the simulation results for the output, control input, feedforward control input, and feedback control input, respectively. Prior to tuning, the tracking performance is poor. Tuning enhances the performance. Although the simulation results (Figures 11(a) and (b), blue lines) are not identical to the actual results (red lines), the estimates are reasonable. This deviation is due to the noise.

Second, a simulation for Case 2 was conducted to evaluate the disturbance suppression performance after parameter tuning using a reference input $r\,(k \geq 0) = 0.0$ and an input disturbance $d\,(k) = 1.0$ as a step signal (step start time is 0.50 s). Figures 12(a)–(c) show the output, control input, and input disturbance, respectively. Prior to tuning,

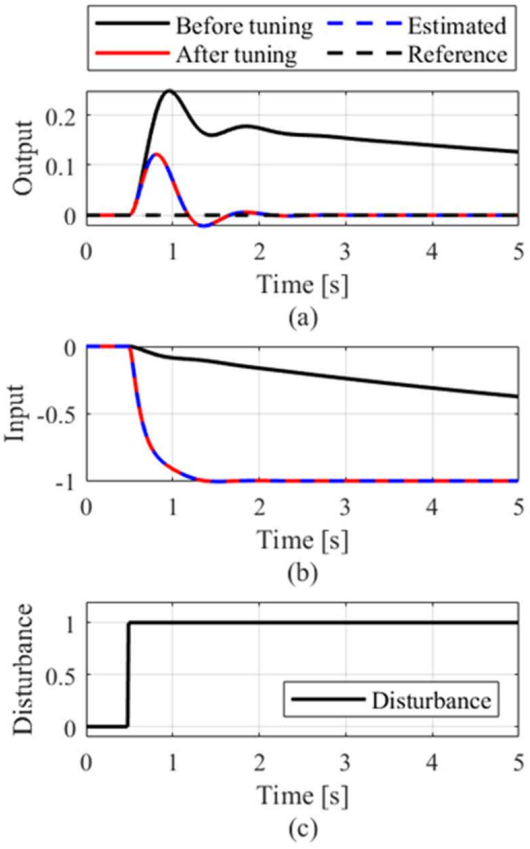

FIGURE 7. Input and output time series data of the disturbance response simulation for Case1. (a) Output, (b) control input, (c) input disturbance.

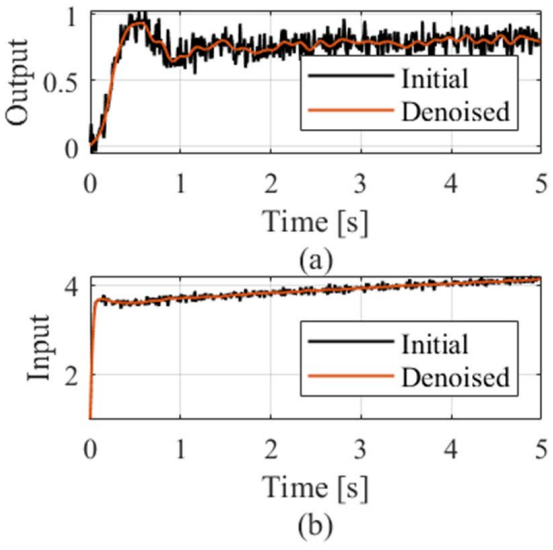

FIGURE 8. Input and output time series data with the initial control parameters in the simulations with/without denoising. (a) Output, (b) input.

the disturbance suppression performance is poor. Tuning enhances the performance. Although the simulation results (Figures 12(a) and (b), blue lines) are not identical to the actual results (red lines), the estimates are reasonable.

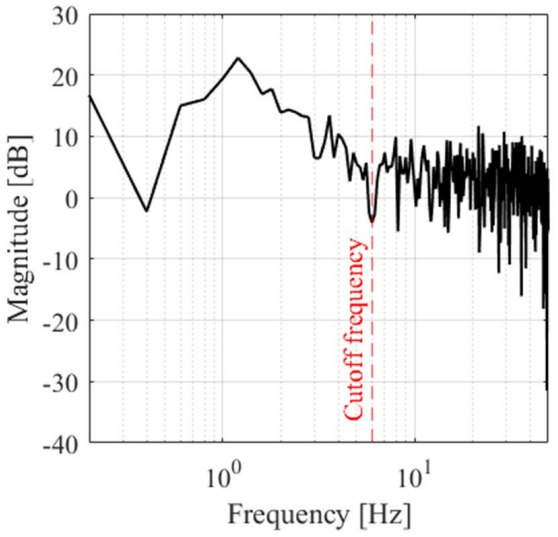

FIGURE 9. Fourier amplitude spectrum of the initial tracking error.

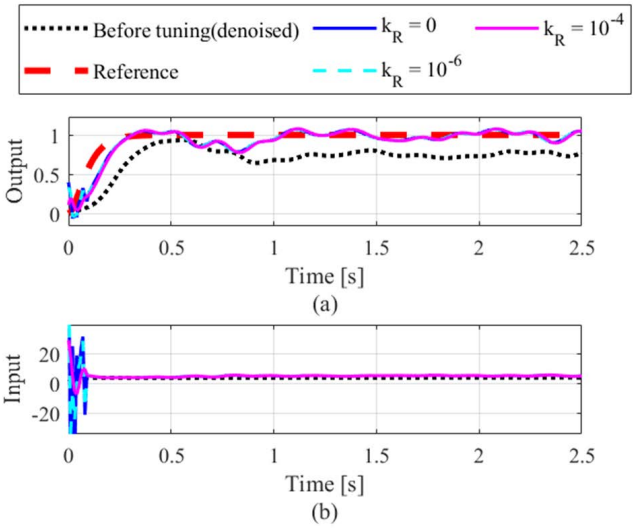

FIGURE 10. Estimated input and output time series data for different k_R in the ridge regression in Case 2. (a) Output, (b) input.

This deviation is due to the noise. It should be noted that tuning increases the value of J_S shown in Table 2 due to the high-frequency noise amplified by the high gain after tuning. However, the step disturbance suppression performance is enhanced (Figure 12). In the noiseless case (Case 1), the objective function value decreases appropriately (Table 1).

C. COMPARISON WITH CONVENTIONAL METHODS

Here, we discuss the differences between the proposed method and other methods.

First, the differences between the proposed method and general model-based design in the control gain optimization method are explained. Model-based design consists of modeling the controlled object (Step 1), designing the control gains based on the obtained model (Step 2), evaluating the

TABLE 2. Control parameters and the value of the objective function in Case 1: Ideal condition.

Symbol		Before tuning	After tuning
Feedback Controller	K_p	+0.2000	+1.9490
	K_i	+0.5000	+19.4375
	K_d	+0.0100	+0.2361
Feedforward Controller	RMS[$\boldsymbol{\theta}$]	0.4834	$\begin{cases}81.486 & k_R = 0\\ 53.785 & k_R = 10^{-6}\\ 12.567 & k_R = 10^{-4}\end{cases}$
Objective function	$\widetilde{J_S}(\boldsymbol{\rho})$	0.5472	2.7482×10^{-3}
	$\widetilde{J_M}(\boldsymbol{\theta})$	0.05961	$\begin{cases}5.663\times10^{-3} & k_R = 0\\ 5.688\times10^{-3} & k_R = 10^{-6}\\ 6.181\times10^{-3} & k_R = 10^{-4}\end{cases}$
	J_S	0.5159	1.1965
	J_M	0.06413	9.300×10^{-3}

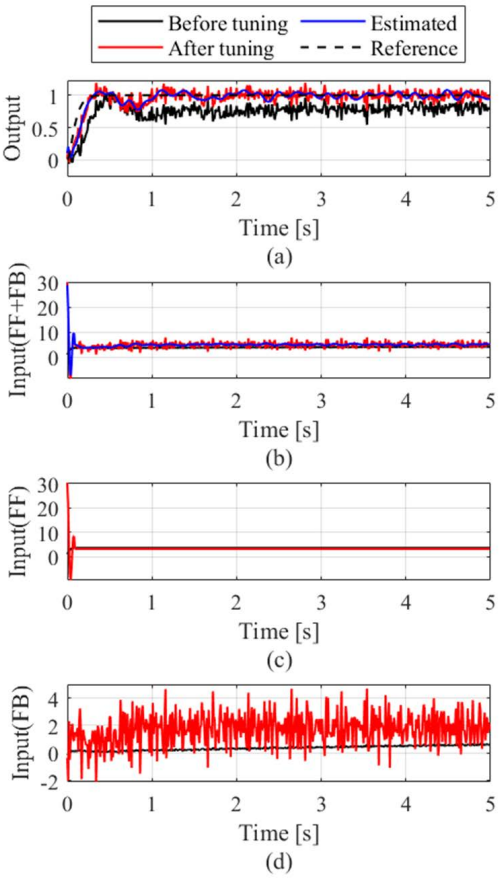

FIGURE 11. Input and output time series data of the set-point response simulation for Case 2. (a) Output, (b) control input, (c) feedforward control input, (d) feedback control input.

control performance on a computer (Step 3), and implementing the control gains (Step 4). In Step 1, the model structure is determined, and the modeling error is evaluated using trial and error. By contrast, this step can be omitted in data-driven control methods, including the proposed method. In Step 3 for general data-driven control methods, the control

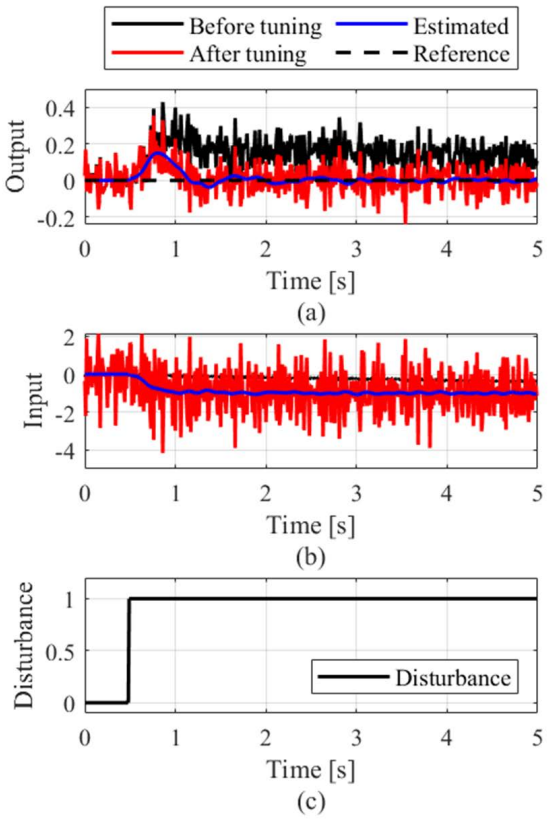

FIGURE 12. Input and output time series data of the disturbance response simulation in Case 2. (a) Output, (b) control input, (c) input disturbance.

gain performance cannot be evaluated until a trial run is completed because the model of the controlled object is unknown. Although the proposed method does not obtain the model of the controlled object, the performance can be evaluated in advance, similar to model-based design.

Effective intelligent algorithm-based controllers have recently been proposed [44], [45]. These methods are applicable to nonlinear MIMO systems and derive control laws with high tracking performances and disturbance resistances. They also consider robustness, stability, and several other constraints. Although they have a wide range of applicability, these methods require information on a nominal model of the controlled object. The proposed method is applied to linear SISO systems, and its two-degree-of-freedom control structure can enhance tracking and disturbance suppression performances. The proposed method does not require information about the controlled object. Furthermore, it can be applied immediately since there is no need to change existing control laws or structures such as PID controllers. Therefore, the proposed method is practical for control plants that cannot be shut down for a long time or in situations where the design cost should be reduced as much as possible.

We also compare the proposed method with conventional DDC methods. In particular, the performances of conventional DDC methods degrade when given a reference model in which model matching is impossible [1], [2].

TABLE 3. Control parameters, values of the objective function, and the gain/phase margins in the comparative simulation.

Symbol		Before tuning	Proposed method	VRFT
Feedback Controller	K_p	+0.2000	+1.4737	-0.6621
	K_i	+0.5000	+17.6447	+33.7321
	K_d	+0.0100	+0.4974	+0.3300
Feedforward Controller	RMS[$\boldsymbol{\theta}$]	0.4834	28.455	483.428
Objective function	$\widetilde{J_S}(\boldsymbol{\rho})$	0.6205	0.05842	233.412
	$\widetilde{J_M}(\boldsymbol{\theta})$	0.08853	0.02451	141.568
	J_{VRFT}	9.5868×10^{-3}	0.01091	8.6249×10^{-3}
	J_M	0.08853	0.02451	141.527
Gain margin [dB]		24.6606	4.3086	-4.6059
Phase margin [degree]		90.5152	51.5177	-64.1660

Here, we perform a comparative simulation of the proposed method with VRFT-2DOF [28], [46], which is a well-known DDC method (see Appendix for the algorithm of VRFT-2DOF). The reference models, controllers, and controlled object are shown in (56–67). The responsivity parameter of the target closed-loop transfer function $M_d(z)$ is $\tau_M = 0.05$, and the time constant of the target sensitivity function $S_d(z)$ is $\tau_S = 0.01$. The dead time of the controlled object is $L = 0.2$. The sampling time T_s is set to 10 ms, and the variance value of white noise $n(k)$ is zero.

Table 3 shows the values before and after tuning the feedback control parameters, root-mean-square of the feedforward control parameters, objective function, and the gain/phase margins. The initial filter coefficient $\boldsymbol{\theta}^{\mathbf{0}}$ of the feedforward controller is shown in (68). The ridge regression parameter is $k_R = 10^{-4}$. Figure 13 shows the response and control input with input disturbance $d(k) = 0$ and step reference input $r(k) = 1.0$. Although the objective function J_{VRFT} decreases when using VRFT, the response is divergent (Table 3 and Figure 13). The gain/phase margin values are both negative, indicating that the closed-loop system is unstable. By contrast, the control gain obtained by the proposed method stabilizes the closed-loop system even when model matching is impossible. Thus, the proposed method, which is based on the ID-FRIT [1], [2] framework can obtain suitable parameters that ensure the stability of the closed-loop BIBO.

V. EXPERIMENTAL VALIDATION

The effectiveness of the proposed method was verified experimentally. The controlled object is a DC motor, where its speed is controlled. Figure 14 overviews the experimental setup. There are two motors connected by a rubber tube: one for driving and the other for detecting the rotation speed (generator).

This experiment employed a 2DOF control system as shown in Figure 1, where the control inputs were calculated by the PID controller (feedback controller) shown in (60–62) and the FIR filter–type controller (feedforward controller) shown in (63–65). The filter time constant τ_f of the

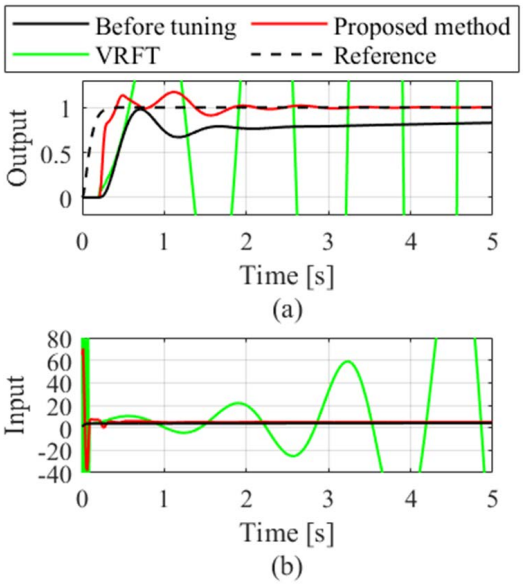

FIGURE 13. Input and output time series data of the set-point response in the comparative simulation. (a) Output, (b) input.

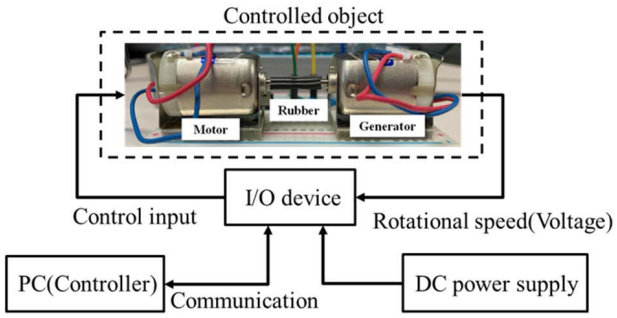

FIGURE 14. Experimental setup.

approximate derivative was set to 0.1. The control input was applied to the drive motor as a voltage value, while the output was the rotational speed (generated voltage) of the other motor connected by a rubber tube. The target closed-loop transfer function $M_d(z)$ employed (56) and (57), and the responsivity parameter was set to $\tau_M = 0.3$. The target sensitivity function $S_d(z)$ employed (58) and (59), and the time constant was set to $\tau_S = 0.15$. The sampling time T_s was 40 ms, and input/output data were obtained from 0.0 to 20.0 s in the initial experiment. Table 2 shows the initial PID gain $\boldsymbol{\rho}^{\mathbf{0}}$ of the feedback section. The initial filter coefficient $\boldsymbol{\theta}^{\mathbf{0}}$ of the feedforward section was set to (68).

Figure 15 shows the initial input/output data and the denoised data. The denoising method was the same as that used in the simulation validation.

Figure 16 shows the DFT result of the initial tracking error $e_{ini}(k)$. The cutoff frequency ω_{k_l} is 1.5 Hz because the noise is dominant above 1.5 Hz. The attenuation rate β in (59) is set to 0.0001. Parameter tuning was conducted using this denoised data (Figure 15, orange line).

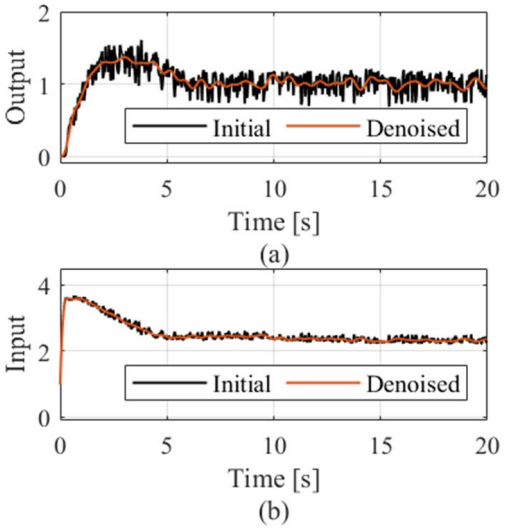

FIGURE 15. Input and output time series of the experimental data using the initial control parameters with/without denoising. (a) Output, (b) input.

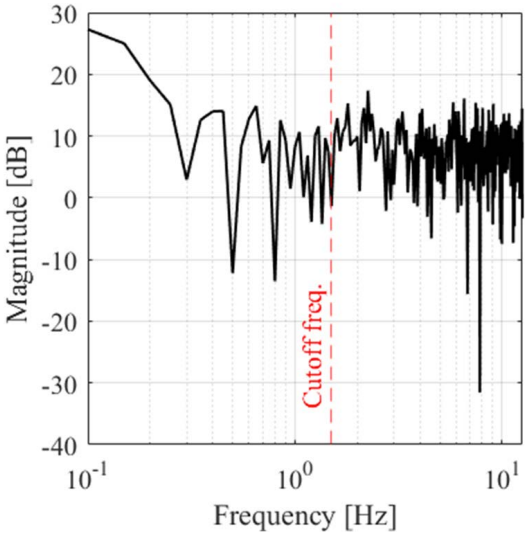

FIGURE 16. Fourier amplitude spectrum of the initial tracking error in the experimental validation.

Table 4 shows the values of the feedback control parameters, root-mean-square of the feedforward control parameters, and objective function before and after tuning. $d^{sup}(k)$ in the feedback control parameter tuning is the step signal with $d^{sup}(k \geq 0) = 1.0$ to suppress a constant value disturbance.

Figure 17 shows the response and control input estimation results from 0.00 to 10.00 s after tuning calculated by (43) and (45) with the different ridge regression parameters k_R described in section III-B, a step reference input $r(k \geq 0) = 1.0$, and an assumed input disturbance $\hat{d}(k) = 0.0$. $k_R = 0, 10^{-5}$, and 10^{-2}.Table 3 shows that the norm of the tuning parameter of the feedforward controller is smaller when ridge regression is used ($k_R = 10^{-5}, 10^{-2}$). The estimated responses are similar when $k_R > 0$. However, the estimated control input can be prevented from becoming too large by

TABLE 4. Control parameters and the value of the objective function in the experimental validation.

Symbol		Before tuning	After tuning
Feedback Controller	K_p	+0.5000	+2.6633
	K_i	+1.0000	+5.1845
	K_d	+0.0100	+0.0939
Feedforward Controller	RMS[$\boldsymbol{\theta}$]	0.4834	$\begin{cases} 35.557 & k_R = 0 \\ 10.771 & k_R = 10^{-5} \\ 1.171 & k_R = 10^{-2} \end{cases}$
Objective function	$\widetilde{J_S}(\boldsymbol{\rho})$	0.05863	0.01413
	$\widetilde{J_M}(\boldsymbol{\theta})$	0.01751	$\begin{cases} 1.634\times10^{-3} & k_R = 0 \\ 1.660\times10^{-3} & k_R = 10^{-5} \\ 2.511\times10^{-3} & k_R = 10^{-2} \end{cases}$
	J_S	0.2467	0.2093
	J_M	0.04827	0.01721

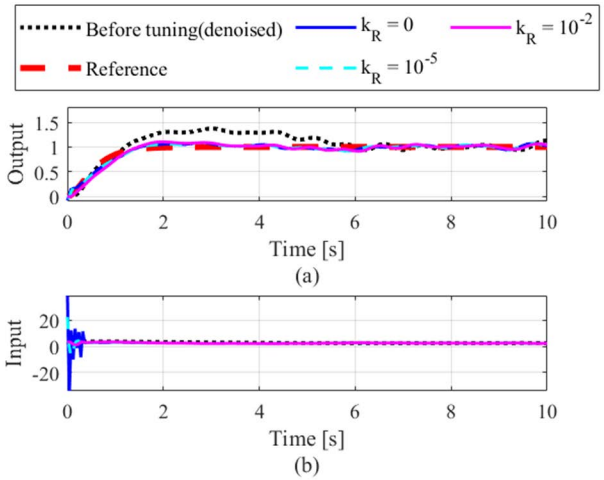

FIGURE 17. Estimated input and output time series data in the experimental validation with different k_R values in the ridge regression. (a) Output, (b) input.

selecting an appropriate value for k_R. Based on these results, below the effects of the tuning parameters at $k_R = 10^{-2}$ were verified.

First, an experiment was conducted to evaluate the tracking performance after parameter tuning using an input disturbance $d(k) = 0$ and a step reference input $r(k) = 1.0$. Figures 18(a)–(d) show the results from 0.00 to 10.00 s for the output, control input, feedforward control input, and feedback control input, respectively. Tuning enhances the tracking performance. Although the estimated results (blue lines) do not completely match the actual results (red lines) due to noise effects, they are a reasonable estimation.

Second, an experiment was conducted to evaluate the disturbance suppression performance after parameter tuning using a reference input $r(k \geq 0) = 1.0$ and an input disturbance $d(k) = 1.5$ as a step signal (step start time is 12.00 s). Figures 19(a)–(c) show results from 10.00 to 20.00 s for the output, control input, and input disturbance, respectively.

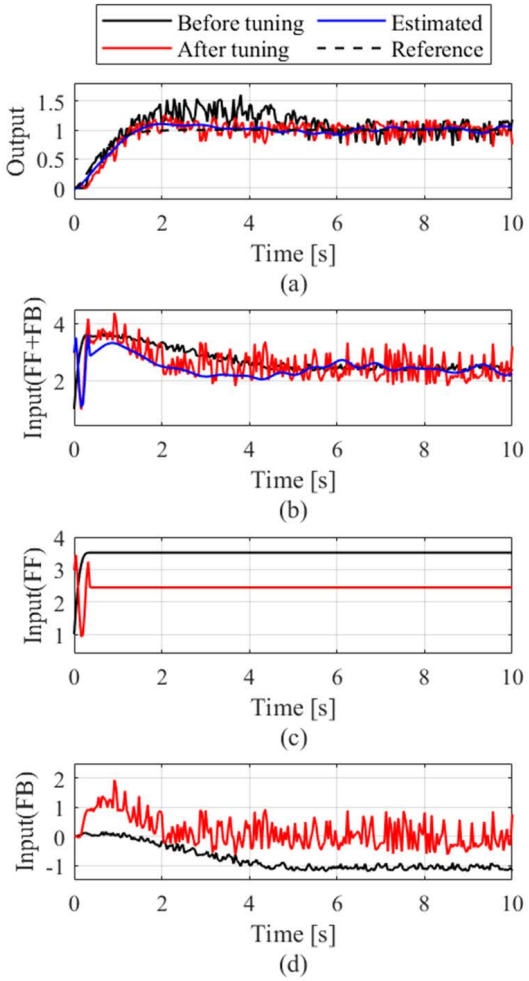

FIGURE 18. Input and output time series of the experimental data in the set-point response. (a) Output, (b) control input, (c) feedforward control input, (d) feedback control input.

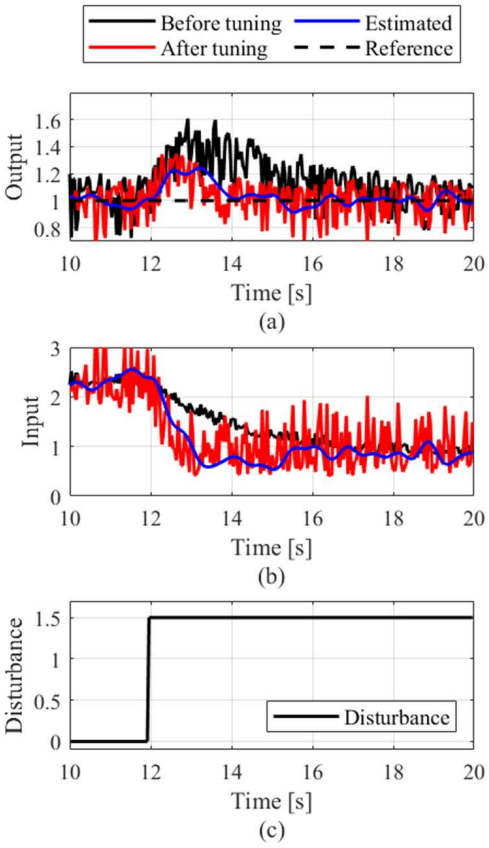

FIGURE 19. Input and output time series of the experimental data in the disturbance response. (a) Output, (b) control input, (c) input disturbance.

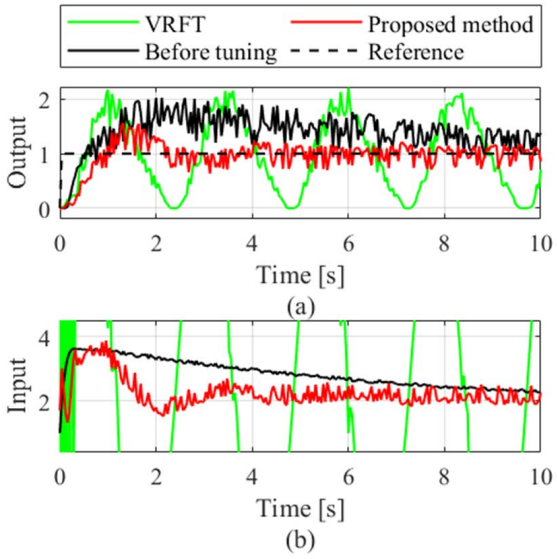

FIGURE 20. Input and output time series data of the set-point response in the comparative experimental validation. (a) Output, (b) input.

Tuning enhances the disturbance suppression performance for step disturbance is enhanced after tuning. Although the estimated results (blue lines) do not completely match the actual results (red lines) due to noise effects, they are a reasonable estimation.

Next, a comparative validation of the proposed method and VRFT-2DOF [28], [46] is performed when model matching with the reference model cannot be realized. The reference models and the controllers are the same, but the responsivity parameter and time constant of the reference models are set to $\tau_M = 0.005$ and $\tau_S = 0.001$, respectively. The sampling time T_s is 40 ms, and the ridge regression parameter is $k_R = 10^{-1}$. The initial input and output data are denoised with a cutoff frequency ω_{k_l} of 2.0 Hz. Table 5 summarizes the simulation results. Figure 20 shows the response and control input with input disturbance $d\,(k) = 0$ and step reference input $r\,(k) = 1.0$. The proposed method can stabilize the closed-loop system even when model matching is impossible. By contrast, the closed-loop system in VRFT does not diverge due to the hardware input voltage limitation from 0 to +5 V. However, the control input is very large, and the tracking performance is deteriorated. These results confirm that the proposed method performs parameter tuning suitable to ensure the stability of the closed-loop BIBO.

TABLE 5. Control parameters and the values of the objective function in the comparative experimental validation.

Symbol		Before tuning	Proposed method	VRFT
Feedback Controller	K_p	+0.1000	+0.8267	-3.4652
	K_i	+0.3000	+5.6203	+24.9062
	K_d	+0.0100	+0.0512	+0.8396
Feedforward Controller	RMS[$\boldsymbol{\theta}$]	0.4834	0.7310	54.088
Objective function	$\widetilde{J_S}(\boldsymbol{\rho})$	0.1683	0.01968	2.9912
	$\widetilde{J_M}(\boldsymbol{\theta})$	0.1298	0.01780	1.9103
	J_{VRFT}	9.6879×10^{-3}	6.5243×10^{-3}	4.5857×10^{-3}
	J_M	0.1549	0.04700	0.46261

VI. CONCLUSION

This study proposes a direct tuning method for the 2DOF controller parameters using only one-shot initial experimental data without mathematical modeling of the controlled object. The proposed method simultaneously enhances the tracking and disturbance suppression performances. Especially, the proposed method can estimate the response and control input after parameter updates without repeated experiments and can take the BIBO stability into account. The obtained optimal parameters are unique and independent of the initial parameters.

In the proposed method, the feedforward and feedback control parameters are tuned by separate calculations. First, the feedback control parameters are tuned to enhance the disturbance suppression performance using the target sensitivity function as an indicator of the disturbance suppression performance. The finite impulse response of a transfer function, whose input and output are respectively the fictitious disturbance signal and the controlled-object input, is identified in the time domain to estimate the response of the sensitivity function. The optimal feedback control parameters are calculated using this estimated response. Then the feedforward control parameters are tuned to enhance the tracking performance using the target closed-loop transfer function as an indicator of the tracking performance. The finite impulse response of a transfer function, whose respective input and output are the fictitious disturbance signal and the controlled-object output, is identified in the time domain to estimate the response of the closed-loop transfer function. If the feedforward controller is parameterized by a linear function of the control parameters, the optimal parameters can be calculated by the least-squares method. The obtained finite impulse response of the closed-loop transfer function can estimate the response and the control input after updating the feedback and feedforward control parameters. This allows the effect of parameter tuning to be evaluated in advance with a computer. Thus, the proposed method leads to efficient control system design.

To validate the effectiveness of the proposed method, simulations of a mechanical system and experimental validation of motor control were conducted. The optimal control parameters to enhance both the tracking and disturbance suppression performances can be obtained for a 2DOF control system. Furthermore, the proposed method accurately estimates the response and control input after updating the tuning parameters using an offline calculation before the parameters are implemented.

Here, the proposed method is applied only to linear SISO systems. To expand the applicable range, our method should be extended to MIMO systems and nonlinear control. One feature of the proposed method is that it can estimate the response and control input after updating the control gains. We plan to investigate a method that considers overshoot and input constraints by adding a constraint term to the objective function using estimated data. We also plan to construct a method to redesign the reference model considering the time delay and the order of the controlled object.

APPENDIX

Here, the procedure of VRFT for 2DOF control system (Figure 1) [28], [46] is briefly described below. It was used as a comparative validation method for sections IV and V.

[Step 0] The designer sets the reference models for the closed-loop transfer function and sensitivity function as $M_d(z)$ and $S_d(z)$, respectively. The object function for the model matching problem is given as

$$J_{MR}(\boldsymbol{\rho},\boldsymbol{\theta}) = \|(T(z,\boldsymbol{\rho},\boldsymbol{\theta}) - M_d(z))W_M(z)\|_2^2 + \|(S(z,\boldsymbol{\rho}) - S_d(z))W_S(z)\|_2^2 \quad (70)$$

$$T(z,\boldsymbol{\rho},\boldsymbol{\theta}) = \frac{G(z)(C_r(z,\boldsymbol{\theta}) + C_e(z,\boldsymbol{\rho})M_d(z))}{1 + G(z)C_e(z,\boldsymbol{\rho})} \quad (71)$$

$$S(z,\boldsymbol{\rho}) = \frac{1}{1 + G(z)C_e(z,\boldsymbol{\rho})} \quad (72)$$

where $W_M(z)$ and $W_S(z)$ are weighting functions chosen by the designer, and controlled object $G(z)$ is unknown.

[Step 1] Acquire input and output data of the controlled object $u_{ini}(k)$, $y_{ini}(k)$, $k = 1, \cdots, N$ in a test.

[Step 2] Construct the virtual reference $\bar{r}(k)$ and the virtual disturbance $\bar{d}(k)$ as

$$M_d(z)\bar{r}(k) = y_{ini}(k) \quad (73)$$

$$S_d(z)\bar{d}(k) = y_{ini}(k) + \bar{d}(k) \quad (74)$$

[Step 3] Construct the virtual input and output data $\bar{u}(k)$, $\bar{y}(k)$, as

$$\bar{y}(k) = y_{ini}(k) + \bar{d}(k) \quad (75)$$

$$\bar{u}(k,\boldsymbol{\theta}) = C_r(z,\boldsymbol{\theta})\bar{r}(k) + C_e(z,\boldsymbol{\rho})(M_d(z)\bar{r}(k) - y_{ini}(k)) = C_r(z,\boldsymbol{\theta})\bar{r}(k) \quad (76)$$

[Step 4] Consider the following objective function J_{VR}^N based on the virtual data and determine the optimal parameters to minimize J_{VR}^N

$$J_{VR}^N(\boldsymbol{\rho},\boldsymbol{\theta}) = \frac{1}{N}\sum_{k=0}^{N-1}\{L_M(z)(u_{ini}(k) - \bar{u}(k,\boldsymbol{\theta}))\}^2$$

$$+\frac{1}{N}\sum_{k=0}^{N-1}\left\{L_S\left(z\right)\left(u_{ini}\left(k\right)+C_e\left(z,\boldsymbol{\rho}\right)y_{ini}\left(k\right)\right)\right\}^2 \tag{77}$$

where $L_M(z)$ and $L_S(z)$ are prefilters. The minimum arguments of $J_{VR}^N(\boldsymbol{\rho},\boldsymbol{\theta})$ and $J_{MR}(\boldsymbol{\rho},\boldsymbol{\theta})$ can be made close to each other by selecting suitable prefilters [28], [46]. Here, $L_M(z)$ and $L_S(z)$ are set as

$$|L_M|^2 = |M_d|^2|S_d|^2|W_M|^2\frac{1}{\Phi_u} \tag{78}$$

$$|L_S|^2 = |S_d-1|^2|S_d|^2|W_S|^2\frac{1}{\Phi_u} \tag{79}$$

where Φ_u is the power spectral density of the initial input data $u_{ini}(k)$. In sections IV and V, the weighting functions are set as

$$W_M(z) = W_S(z) = \frac{1}{1-z^{-1}} \tag{80}$$

(80) is given as an integrator, which is appropriate because the reference signal and the input disturbance are step signals. This paper uses the denoising data $u_f^*(k)$ and $y_f^*(k)$ from section III-D instead of $u_{ini}(k)$ and $y_{ini}(k)$ in the noisy condition.

REFERENCES

[1] S. Yahagi and I. Kajiwara, "Direct tuning of the data-driven controller considering closed-loop stability based on a fictitious reference signal," *Meas. Control*, vol. 54, nos. 5–6, pp. 1026–1042, May 2021, doi: 10.1177/00202940211010834.
[2] S. Yahagi and I. Kajiwara, "Direct tuning of PID controller and reference model with input constraint," in *Proc. 21st Int. Conf. Control, Autom. Syst. (ICCAS)*, Oct. 2021, pp. 1424–1429, doi: 10.23919/ICCAS52745.2021.9649821.
[3] A. Yonezawa, H. Yonezawa, and I. Kajiwara, "Parameter tuning technique for a model-free vibration control system based on a virtual controlled object," *Mech. Syst. Signal Process.*, vol. 165, Feb. 2022, Art. no. 108313, doi: 10.1016/j.ymssp.2021.108313.
[4] Z. Hou and S. Jin, "Data-driven model-free adaptive control for a class of MIMO nonlinear discrete-time systems," *IEEE Trans. Neural Netw.*, vol. 22, no. 12, pp. 2173–2188, Dec. 2011, doi: 10.1109/TNN.2011.2176141.
[5] Z.-S. Hou and Z. Wang, "From model-based control to data-driven control: Survey, classification and perspective," *Inf. Sci.*, vol. 235, pp. 3–35, Jun. 2013, doi: 10.1016/j.ins.2012.07.014.
[6] S. Yahagi and I. Kajiwara, "Non-iterative data-driven tuning of model-free control based on an ultra-local model," *IEEE Access*, vol. 10, pp. 72773–72784, 2022, doi: 10.1109/ACCESS.2022.3188713.
[7] K. Prag, M. Woolway, and T. Celik, "Data-driven model predictive control of DC-to-DC buck-boost converter," *IEEE Access*, vol. 9, pp. 101902–101915, 2021, doi: 10.1109/ACCESS.2021.3098169.
[8] K. Deng, F. Li, and C. Yang, "A new data-driven model-free adaptive control for discrete-time nonlinear systems," *IEEE Access*, vol. 7, pp. 126224–126233, 2019, doi: 10.1109/ACCESS.2019.2938998.
[9] K. Prag, M. Woolway, and T. Celik, "Toward data-driven optimal control: A systematic review of the landscape," *IEEE Access*, vol. 10, pp. 32190–32212, 2022, doi: 10.1109/ACCESS.2022.3160709.
[10] H. Hjalmarsson, M. Gevers, S. Gunnarsson, and O. Lequin, "Iterative feedback tuning: Theory and applications," *IEEE Control Syst.*, vol. 18, no. 4, pp. 26–41, Aug. 1998, doi: 10.1109/37.710876.
[11] L. Mišković, A. Karimi, D. Bonvin, and M. Gevers, "Correlation-based tuning of decoupling multivariable controllers," *Automatica*, vol. 43, no. 9, pp. 1481–1494, Sep. 2007, doi: 10.1016/j.automatica.2007.02.006.
[12] A. Karimi, K. van Heusden, and D. Bonvin, "Non-iterative data-driven controller tuning using the correlation approach," in *Proc. Eur. Control Conf. (ECC)*, Jul. 2007, pp. 5189–5195, doi: 10.23919/ecc.2007.7068802.
[13] G. O. Guardabassi and S. M. Savaresi, "Virtual reference direct design method: An off-line approach to data-based control system design," *IEEE Trans. Autom. Control*, vol. 45, no. 5, pp. 954–959, May 2000, doi: 10.1109/9.855559.
[14] M. C. Campi, A. Lecchini, and S. M. Savaresi, "Virtual reference feedback tuning: A direct method for the design of feedback controllers," *Automatica*, vol. 38, no. 8, pp. 1337–1346, Aug. 2002, doi: 10.1016/S0005-1098(02)00032-8.
[15] M. C. Campi and S. M. Savaresi, "Direct nonlinear control design: The virtual reference feedback tuning (VRFT) approach," *IEEE Trans. Autom. Control*, vol. 51, no. 1, pp. 14–27, Jan. 2006, doi: 10.1109/TAC.2005.861689.
[16] O. Kaneko, "Data-driven controller tuning: FRIT approach," *IFAC Proc. Volumes* vol. 46, no. 11, pp. 326–336, 2013, doi: 10.3182/20130703-3-FR-4038.00122.
[17] S. Yahagi, I. Kajiwara, and T. Shimozawa, "Slip control during inertia phase of clutch-to-clutch shift using model-free self-tuning proportional-integral-derivative control," *Proc. Inst. Mech. Eng., D, J. Automobile Eng.*, vol. 234, no. 9, pp. 2279–2290, Aug. 2020, doi: 10.1177/0954407020907257.
[18] M. Kano and M. Ogawa, "The state of the art in chemical process control in Japan: Good practice and questionnaire survey," *J. Process Control*, vol. 20, no. 9, pp. 969–982, Oct. 2010, doi: 10.1016/j.jprocont.2010.06.013.
[19] R. N. Tripathi and T. Hanamoto, "FRIT based optimized PI tuning for DC link voltage control of grid connected solar PV system," in *Proc. 41st Annu. Conf. IEEE Ind. Electron. Soc.*, Nov. 2015, pp. 1567–1572, doi: 10.1109/IECON.2015.7392324.
[20] J. Rojas, X. Flores-Alsina, U. Jeppsson, and R. Vilanova, "Application of multivariate virtual reference feedback tuning for wastewater treatment plant control," *Control Eng. Pract.*, vol. 20, no. 5, pp. 499–510, 2012, doi: 10.1016/j.conengprac.2012.01.004.
[21] T. E. Passenbrunner, S. Formentin, S. M. Savaresi, and L. del Re, "Direct multivariable controller tuning for internal combustion engine test benches," *Control Eng. Pract.*, vol. 29, pp. 115–122, Aug. 2014, doi: 10.1016/j.conengprac.2014.04.009.
[22] S. Yahagi and I. Kajiwara, "Direct tuning of gain-scheduled controller for electro-pneumatic clutch position control," *Adv. Mech. Eng.*, vol. 13, no. 8, pp. 1–12, 2021, doi: 10.1177/16878140211036017.
[23] S. Formentin, G. Panzani, and S. M. Savaresi, "VRFT for LPV systems: Theory and braking control application," in *Robust Control and Linear Parameter Varying Approaches* (Lecture Notes in Control and Information Sciences), vol. 437. Heidelberg, Germany: Springer-Verlag, 2013, pp. 289–309, doi: 10.1007/978-3-642-36110-4_11.
[24] K. van Heusden, A. Karimi, D. Bonvin, A. den Hamer, and M. Steinbuch, "Non-iterative data-driven controller tuning with guaranteed stability: Application to direct-drive pick-and-place robot," in *Proc. IEEE Int. Conf. Control Appl.*, Sep. 2010, pp. 1005–1010, doi: 10.1109/CCA.2010.5611118.
[25] L. Duan, Z. Hou, X. Yu, S. Jin, and K. Lu, "Data-driven model-free adaptive attitude control approach for launch vehicle with virtual reference feedback parameters tuning method," *IEEE Access*, vol. 7, pp. 54106–54116, 2019, doi: 10.1109/ACCESS.2019.2912902.
[26] O. Kaneko, Y. Yamashina, and S. Yamamoto, "Fictitious reference tuning of the feed-forward controller in a two-degree-of-freedom control system," *SICE J. Control, Meas., Syst. Integr.*, vol. 4, no. 1, pp. 55–62, Jan. 2011, doi: 10.9746/jcmsi.4.55.
[27] T. Sakata, O. Kaneko, and T. Fujii, "Parameter tuning of two-degree of freedom controllers using FRIT for the tracking property and the feedback properties," *Trans. Inst. Syst., Control Inf. Eng.*, vol. 20, no. 11, pp. 419–429, 2007, doi: 10.5687/iscie.20.419.
[28] A. Lecchini, M. C. Campi, and S. M. Savaresi, "Virtual reference feedback tuning for two degree of freedom controllers," in *Proc. Eur. Control Conf. (ECC)*, Sep. 2001, pp. 2416–2421, doi: 10.23919/ECC.2001.7076288.
[29] T. Ikezaki and O. Kaneko, "A new approach of data-driven controller tuning method by using virtual IMC structure—Virtual internal model tuning," *IFAC-PapersOnLine*, vol. 52, no. 29, pp. 344–349, 2019, doi: 10.1016/j.ifacol.2019.12.699.
[30] T. Ikezaki and O. Kaneko, "Data-driven update of two-degree-of-freedom control system by virtual internal model tuning," *Trans. Soc. Instrum. Control Eng.*, vol. 56, no. 3, pp. 98–105, 2020, doi: 10.9746/sicetr.56.98.
[31] Y. Fujimoto, "Estimated response iterative tuning with signal projection," *IFAC J. Syst. Control*, vol. 19, Mar. 2022, Art. no. 100179, doi: 10.1016/j.ifacsc.2021.100179.

[32] O. Kaneko and T. Nakamura, "Data-driven prediction of 2DOF control systems with updated feedforward controller," in *Proc. 56th Annu. Conf. Soc. Instrum. Control Eng. Jpn. (SICE)*, Sep. 2017, pp. 259–262, doi: 10.23919/SICE.2017.8105636.
[33] O. Kaneko, T. Nakamura, and T. Ikezaki, "A new approach to update of feedfoward controller in the two-degree-of-freedom control system—A proposal of estimated response iterative tuning (ERIT)," *Trans. Soc. Instrum. Control Eng.*, vol. 54, no. 12, pp. 857–864, 2018, doi: 10.9746/sicetr.54.857.
[34] T. Sakatoku, K. Yubai, D. Yashiro, and S. Komada, "Data-driven controller tuning with closed-loop response estimation," *IEEJ Trans. Electr. Electron. Eng.*, vol. 16, no. 10, pp. 1397–1406, Oct. 2021, doi: 10.1002/TEE.23436.
[35] M. G. Safonov and T.-C. Tsao, "The unfalsified control concept and learning," *IEEE Trans. Autom. Control*, vol. 42, no. 6, pp. 843–847, Jun. 1997, doi: 10.1109/9.587340.
[36] T. Hori, K. Yubai, D. Yashiro, and S. Komada, "Data-driven controller tuning for sensitivity minimization," in *Proc. Int. Conf. Adv. Mech. Syst. (ICAMechS)*, Nov. 2016, pp. 132–137, doi: 10.1109/ICAMechS.2016.7813434.
[37] M. Kosaka, A. Kosaka, and M. Kosaka, "Virtual time-response based iterative gain evaluation and redesign," *IFAC-PapersOnLine*, vol. 53, no. 2, pp. 3946–3952, 2020, doi: 10.1016/j.ifacol.2020.12.2249.
[38] S. Ichinomoto and M. Kuramoto, "V-tiger for 2-degree of freedom control system," in *Proc. Jpn. Jt. Autom. Control Conf.*, vol. 63, 2020, pp. 1265–1272, doi: 10.11511/jacc.63.0_1265.
[39] N. Hansen, "The CMA evolution strategy: A tutorial," 2016, *arXiv:1604.00772*.
[40] Y. Wakasa, S. Kanagawa, K. Tanaka, and Y. Nishimura, "FRIT for systems with dead-zone and its application to ultrasonic motors," *IEEJ Trans. Electron., Inf. Syst.*, vol. 131, no. 6, pp. 1209–1216, 2011, doi: 10.1541/IEEJEISS.131.1209.
[41] A. E. Hoerl and R. W. Kennard, "Ridge regression: Biased estimation for nonorthogonal problems," *Technometrics*, vol. 12, no. 1, pp. 55–67, 1970, doi: 10.1080/00401706.1970.10488634.
[42] A. E. Hoerl and R. W. Kennard, "Ridge regression: Applications to nonorthogonal problems," *Technometrics*, vol. 12, no. 1, pp. 69–82, 1970, doi: 10.1080/00401706.1970.10488635.
[43] Y. Matsui, H. Ayano, S. Masuda, and K. Nakano, "A controller tuning method based on finite impulse response estimation using closed-loop response data," *IEEJ Trans. Electron., Inf. Syst.*, vol. 139, no. 8, pp. 858–865, Aug. 2019, doi: 10.1541/IEEJEISS.139.858.
[44] T. Yang, N. Sun, and Y. Fang, "Neuroadaptive control for complicated underactuated systems with simultaneous output and velocity constraints exerted on both actuated and unactuated states," *IEEE Trans. Neural Netw. Learn. Syst.*, early access, Oct. 8, 2021, doi: 10.1109/TNNLS.2021.3115960.
[45] T. Yang, N. Sun, H. Chen, and Y. Fang, "Adaptive optimal motion control of uncertain underactuated mechatronic systems with actuator constraints," *IEEE/ASME Trans. Mechatronics*, early access, Aug. 9, 2022, doi: 10.1109/TMECH.2022.3192002.
[46] J. D. R. Fernandez, "Extensions and applications of the virtual reference feedback tuning," Ph.D. dissertation, Dept. Telecom. Syst. Eng., Autonomous Univ. Barcelona, Barcelona, Spain, 2011.

TATSUNARI SAKAI received the B.S. degree in mechanical engineering from Hokkaido University, Japan, in 2021, where he is currently pursuing the M.S. degree with the Graduate School of Engineering. His research interests include data-driven control, two-degree-of freedom control, and adaptive control.

SHUICHI YAHAGI received the B.S. degree in engineering from the Shibaura Institute of Technology, Japan, in 2011, and the M.S. and Ph.D. degrees in engineering from Hokkaido University, Japan, in 2013 and 2021, respectively. In 2013, he joined the ISUZU Advanced Engineering Center, Ltd. He is currently a Senior Research Engineer at the 6th Research Department, ISUZU Advanced Engineering Center, Ltd. His research interests include automobile control, data-driven control, model-free control, and PID control. His research has led to over 20 patents.

ITSURO KAJIWARA received the B.S. degree in engineering from Tokyo Metropolitan University, in 1986, and the M.S. and Ph.D. degrees in engineering from the Tokyo Institute of Technology, in 1988 and 1993, respectively. From 1990 to 2000, he was an Assistant Professor with the School of Engineering, Tokyo Institute of Technology. From 2000 to 2008, he was an Associate Professor with the Graduate School of Engineering, Tokyo Institute of Technology. Since 2009, he has been a Professor with the Graduate School of Engineering, Hokkaido University. His research interests include vibration, control, structural health monitoring, and laser application.